Hydrolysable bio-based polyhydroxyurethane networks with shape memory behavior at body temperature

Fiona Magliozzi, Arthur Scali, Guillaume Chollet, Damien Montarnal, Etienne Grau, Henri Cramail

Hydrolysable bio-based polyhydroxyurethane networks with shape memory behavior at body temperature

Fiona Magliozzi[1], Arthur Scali[1], Guillaume Chollet[3], Damien Montarnal[2*], Etienne Grau[1*], Henri Cramail[1*]

[1]Univ. Bordeaux, CNRS, Bordeaux INP, LCPO, UMR 5629, F-33600, Pessac, France

[2]Univ Lyon, Université Claude Bernard Lyon 1, CPE Lyon, CNRS, UMR 5265, C2P2, 43 Bvd. du 11 Novembre 1918, F-69616 Villeurbanne, France

[3]ITERG, 11 rue Gaspard Monge, 33610 Canéjan, France

ABSTRACT

Among possible routes towards isocyanate-free PUs, aminolysis of cyclic carbonates leading to polyhydroxyurethanes (PHUs) is one of the most promising pathways. Herein, we describe the solvent-free synthesis of shape memory PHU networks from diglycerol dicarbonate through reactive extrusion with varying amounts of primary and secondary triamines, Tris(2-aminoethyl)amine and Tris(2-(methylamino)ethyl)amine). Depending on the composition of the system, the glass transition temperature of the PHU networks can be finely tuned in the 20-40°C range and, consequently, affords shape memory recovery at body temperature. In addition, these networks revealed hydrolysable over a few months and may find uses as bioresorbable templates for medical applications.

INTRODUCTION

Polyhydroxyurethanes (PHUs) resulting from the polyaddition of cyclic carbonates and polyamines and bearing hydroxyl moieties on their backbone appear to be the most promising candidates to replace conventional isocyanate-based PUs.[1] Despite the numerous advantages shown by this synthetic route, added to the possibility to use bio-based monomers, the valorization of PHUs is still suffering from some limitations. In particular, the reaction extent is generally incomplete, leading to PHUs with limited molar masses and insufficient mechanical properties. In solvent-free polymerizations, the viscosity issues are partly responsible for the slow kinetics, as mentioned in several publications.[2–6] To circumvent this limitation, we recently evidenced the benefit brought by the reactive extrusion process towards PHUs solvent-free syntheses.[7] The process allowed for the synthesis of a series of PHU materials in short reaction times, even from high viscosity reactive precursors.

Considering the fact that reactive extrusion stands for a promising tool to make solvent-free PHUs materials, we investigated the synthesis of PHU networks that could be easily generated and recovered. In this work, PHU networks exhibiting shape memory features were investigated.

Shape memory polymers (SMPs) are a class of materials developed for many applications[8] including shrink films for packaging[9], self-deployable structures in aerospace devices,[10,11] smart textiles[12,13] sensors and actuators[14], flexible substrates for electronic devices[15] to a large number of biomedical applications, like self-tightenable suture or implants for minimal invasive surgery[16]. Most of SMPs are dual-shape memory polymers (dual-SMPs) in which a three dimensional chemical or physical network determines a permanent shape A in stress-free conditions and an additional reversible transition (glass transition, crystallization) induces a strong increase of the material stiffness and the fixing of a temporary shape B.[17] The typical shape-B fixing procedure consists thus in tensioning or bending the SMP while cooling below the glass transition or crystallization temperatures. Shape-A recovery readily occurs when an external stimulus (e.g. heat, light[18], magnetic[19] fields) is applied, and residual stresses can effectively relax to yield shape B (Additional explanation in SI, Figure SI.1). According to our knowledge, the literature regarding PHUs exhibiting shape memory property is relatively scarce. In 2017, Mülhaupt and coll. described the thermoresponsive triple shape memory behavior of polyethyleneimine (PEI)/behenic acid-based PHUs. By exploiting the glass transition temperature (T_g = 25 - 40 °C), the crystallization of the long aliphatic segments (T_m = 40 – 75 °C) and the presence of a cross-linked network, two temporary shapes could be successively stored and recovered.[4]

Building on the previous developments of bio-based PHUs from glycerol dicarbonate (DGDC) and various amines,[20–23] we report in this manuscript the solvent-free syntheses of cross-linked PHUs by reactive extrusion between DGDC and varying amounts of primary and secondary triamines, tris(2-aminoethyl)amine, TAEA and tris(2-(methylamino)ethyl)amine, TMAEA, respectively. Depending on the composition of these PHUs, their T_g can be finely tuned in the 20-40 °C range and their properties as SMP were evaluated. In order to investigate more specifically the aptitude of these systems for potential biomedical applications, we investigated shape recovery at body temperature (37 °C). Finally, the capacity of these PHUs to degrade by hydrolysis was also demonstrated, that suggests interesting bioresorbable abilities that may yet to be fully investigated in regard to cytotoxicity of the degradation byproducts.

EXPERIMENTAL SECTION

Materials

Diglycerol, Tris(2-aminoethyl)amine (TAEA) and Tris(2-(methylamino)ethyl)amine (TMAEA) were purchased from TCI Chemicals, Europe. Sodium methoxide (NaMeO) was provided by Alfa Aesar. Dimethylcarbonate (DMC, extra dry, 99 %), was obtained from Acros. Deuterated solvents such as D_2O and DMSO-d6 were purchased from Eurisotop. THF and DMF were provided by VWR company. Hexylamine was obtained from Sigma Aldrich.

Methods and instruments

Nuclear Magnetic Resonance. ^{1}H nuclear magnetic resonance (NMR) spectra were recorded on a Bruker ADVANCE 400 spectrometer (400.20 MHz) using DMSO-d6 or D_2O as a solvent at 25 °C.
Size Exclusion Chromatography. Polymer molar masses were determined by size exclusion chromatography (SEC) using DMF (DMF + lithium bromide LiBr 1 g.L^{-1}) as the eluent. Measurements in DMF were performed on an UltiMate 3000 system from Thermoscientific equipped with diode array detector DAD. The system also includes a multiangle light scattering detector MALLS and differential refractive index detector dRI from Wyatt Technology. Polymers were separated on two GF310 + 510 Asahipak columns containing a polyvinyl alcohol phase (7.5 × 300, exclusion limit: 300 000 g mol^{-1}). Column's temperature was held at 50 °C. Polystyrene was used as the standard and the calibration method is conventional.
Thermogravimetric Analyses. Thermogravimetric analyses (TGAs) were performed on the TGA-Q500 system from TA Instruments at a heating rate of 10 °C min^{-1} under a nitrogen atmosphere from room temperature to 600 °C and then under air atmosphere from 600 to 700 °C.

Differential Scanning Calorimetry. Differential scanning calorimetry (DSC) thermograms were measured using a DSC Q100 apparatus from TA Instruments. For each sample, two cycles were performed, the first from −40 to 180 °C at 10 °C min^{-1} and a second from −40 to 180 °C. The glass transition and melting temperatures were calculated from the second heating run.
Compounder (Twin-Screw Extruder). As previously published by our group[7], the reactive compounding was performed using a Micro 5/14 mm twin-screw compounder from Thermos Scientific, at a temperature of 90 °C. The rotation speed of the twin screw was kept constant at 100 rpm.

Fourier Transform Infrared Spectroscopy. Infrared spectra were obtained on a Bruker-Tensor 27 spectrometer, equipped with a diamond ATR cell. The spectra were acquired from 400 to 4000 cm^{-1} using 64 scans at a resolution of 4 cm^{-1}.

DGDC Synthesis. DGDC was synthesized according to the previously reported synthesis.[7] DGDC was prepared from diglycerol with a 40 % yield through a one-step procedure. In a round-bottom flask, 76 g (1 eq.) of diglycerol were introduced and dried under vacuum during 2 h at 90 °C. Then, nitrogen was flushed into the vessel and 1.24 g (0.05 eq.) of sodium methoxide catalyst was added under stirring. A condenser was set up above the flask and 5 eq. (231 mL) of the second reactant, DMC, was added. The DMC also plays the role of the reaction solvent. The temperature was then set at 110 °C. After 48 h reaction, the mixture was filtered to remove the sodium methoxide and concentrated by evaporation before two successive recrystallizations in methanol at −80 °C. DGDC was recovered by filtration on paper filters and dried under vacuum at room temperature. ^{1}H NMR (DMSO-d6, 25 °C, 400 MHz): δ (ppm) 4.93 (m, 2H, H2), 4.52 and 4.23 (t, 4H, H1), 3.74 (t, 4H, H3). ^{13}C NMR (DMSO-d6, 25 °C, 100 MHz): δ (ppm) 154.9 (OCOO), 74.8 (CH−CH_2−O−CH_2), 69.8 (CH−CH_2−O−CH_2), 66.1 (CH_2−CH−CH_2−O−CH_2). IR (cm^{-1}): 2925, 1773, 1476, 1401, 1165. T_m = 69 °C.

Standard procedure for polymerization by reactive extrusion process. The extruder is pre-heated at 90 °C and DGDC (powder, 1 eq., 4.6 g) is added in the reactor. The speed of the rotating screws is set at 100 rpm and kept steady during the process. After 1 min 30 seconds, a stoichiometric (1:1 ratio of amine:carbonate) amount of triamine (or primary and secondary triamines mixture) is injected into the reactor with a syringe. When the extruder automatically stops (e.g. when the torque reaches the threshold value of 5 Nm or ΔP reaches 200 bars), the extruder is opened and PHUs, molded into the circulation channel as 9,5 x 63 x 1,5 mm^3 strips, are recovered. The PHUs strips were post-cured at 90 °C between 180 min and 220 min depending on the systems to reach full conversion. Detailed curing procedure is available in Supporting Information, Figure SI-2.

Synthesis of the hydroxyurethane model compound HU-m. DGDC (0.5 g, 1 eq.) and hexylamine (0.6 ml, 2 eq.) were premixed and mechanically stirred during 4 h at 80 °C. The product was directly analyzed by ^{1}H NMR.

Model carbonation of triamines with CO_2. 10 mg of TAEA and TMAEA were solubilized in 500 µL of D_2O and introduced respectively in two NMR tubes. After the initial ^{1}H NMR spectra were recorded, CO_2 at ambient pressure was flushed into the NMR tube during 30 min, at room temperature. Then, the spectra of the carbonated amines were recorded.

Swelling tests. Rectangular pieces of the PHUs (weight m_0) were introduced in closed flasks containing 5 ml of THF and let at room temperature. PHU pieces are then weighted after different times and the obtained mass is labelled m. The swelling ratio is then calculated by the following equation:

$$\text{Swelling ratio (\%)} = \frac{m - m_0}{m_0} \times 100$$

After 70 days in THF, the samples were dried overnight under vacuum and weighted (m_3). Gel contents are then determined according the following equation:

$$\text{Gel content (\%)} = \frac{m_3}{m_0} \times 100$$

Rheometry. Thermomechanical and shape memory characterization of cross-linked PHUs were carried out with a HAAKE MARS 60 rheometer (Thermofisher Scientific) using 8 mm plane geometries on disks punched out from thoroughly dried PHU strips (diameter 8 mm and thickness about 1.5 mm). The different steps of the protocol are detailed in Supporting Information, Table SI-1 and build on a previously developed procedure.[24] The characterization protocol is divided into three parts. After initial thermal equilibration (20 min, 0 °C, normal force Fn = 0.5 N), a first heating ramp was carried out while merely maintaining the sample contact thus accommodating the thermal expansion of the sample (0 °C to 80 °C at 3 °C min^{-1}, F_N = 0.5 N,). In the second part, four compression fixing and recovery cycles were run: i) 5 min equilibration at 80 °C to measure the stress-free height of the sample $h_{0,i}$, ii) 5 min compression at 80°C (F_N = 20 N) leading to a height $h_{1,i}$, iii) cooling ramp from 80 to 0 °C at 3 °C min^{-1} while maintaining the compression, F_N = 20 N iv) release of the compression (F_N=0.5 N) to measure the fixed height $h_{2,i}$ and v) heating ramp from 0 °C to 80 °C at 3 °C min^{-1} while maintaining sample contact (F_N = 0.5 N) and thus monitoring the shape recovery, with final height $h_{3,i}$. During the heating and cooling ramps of these cycles, the application of additional small amplitude oscillatory shear (SAOS, oscillatory stress 1000 Pa, 1 Hz) enables simultaneous dynamic mechanical analysis. In a third part, after fixing the shape as previously described (20 N compression, 0 °C), the shape recovery was monitored over 2 h upon temperature jump at 37 °C.

Thermal expansion. The contribution of thermal expansion $\alpha(T) = h_{stress\ free}(T) \,/\, h_{stress\ free}(10\ °C)$ measured in the first part were taken into account in all subsequent height measurements (See Figures SI-7 and SI-8 in Supporting Information).

Recovery and fixity rate calculation. The recovery rate R_r, describing the capacity of the material to recover the initial shape after the i^{th} cycle is calculated using equation 1.

$$R_{r,i} = \frac{h_{3,i} - h_{1,i}}{h_{0,1} - h_{1,i}} \quad (1)$$

The corresponding fixity rate, describing the capacity of the material to maintain its temporary shape during the i^{th} fixing cycle is calculated using equation 2.

$$R_{f,i} = \frac{h_{0,i} - h_{2,i}}{h_{0,1} - h_{1,i}} \quad (2)$$

RESULTS AND DISCUSSION

DGDC-based cross-linked PHUs synthesized through reactive extrusion.

PHU networks were synthesized through the reactive extrusion polymerization of bio-based diglycerol dicarbonate (DGDC) and two different triamines (tris(2-aminoethyl)amine, TAEA and tris(2-(methylamino)ethyl)amine, TMAEA) while maintaining an overall carbonate:amine stoichiometric ratio of 1 (Figure 1). As expected from the literature,[25] the secondary amines were found to be less reactive than primary amines toward nucleophilic addition on cyclic carbonates, slowing down the overall reaction kinetics. After addition of the triamines in the extruder containing DGDC, the pressure in the recirculation channel, measured by two pressure sensors, progressively increased as the polyaddition occurred. In close proximity of the gel point, as the viscosity reaches extremely high values and the torque considerably increases, the extruder automatically stops. Materials can be recovered as strips molded into the extruder recirculation channel. The PHUs were further cured at 90 °C between 180 min (PHU_0) and 220 min (PHU_{100}) depending on the systems, until the complete consumption of carbonate moieties. Detailed on the curing procedure is available in Figure SI-2.

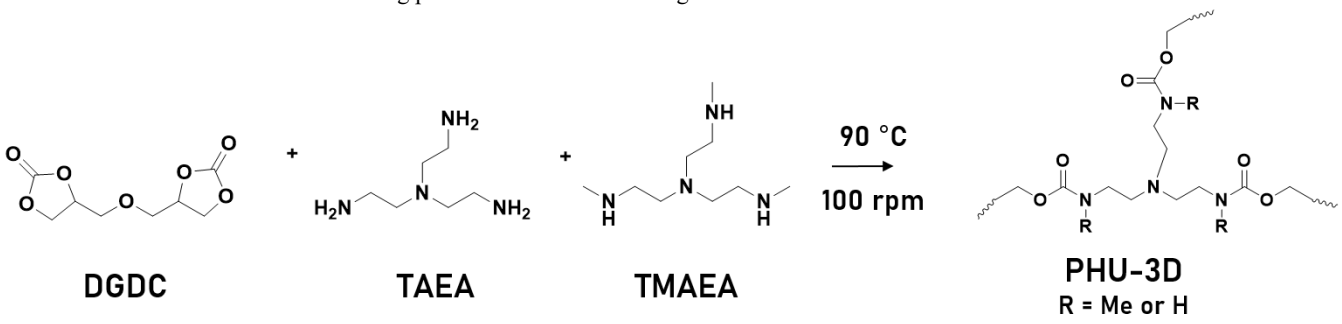

Figure 1. Synthesis of DGDC-based PHUs with triamines.

Following this procedure, 5 cross-linked PHUs have been synthesized, with compositions ranging from 100% TAEA to 100% TMAEA. As expected, the gel times (assimilated to the reaction time before extruder stops) significantly increase with the fraction of TMAEA (Table 1), thus indicating lower reactivity of secondary amines.

Table 1. Gel times for PHUs with different TAEA/TMAEA compositions and physical properties of corresponding fully cured networks.

PHU	TMAEA fraction	Gel time (min)	Swelling rate after 70 days in THF (%)	T_g (°C)[a]	T_{d5} % (°C)[b]	T_α (°C)[c]	G_0 (MPa)[c]	ν_e (mol.m^{-3})[d]
PHU$_0$	0	5.5	0	42	219	32 / 40	2.0	230
PHU$_{30}$	30	8.5	0	34	215	36	1.0	118
PHU$_{50}$	50	15	0	30	217	34	0.91	103
PHU$_{70}$	70	23	4.6	26	216	28	0.45	51
PHU$_{100}$	100	45	15	20	214	21	0.27	30

[a] Determined from DSC second heating cycle, 10 °C min^{-1}. [b] Determined from TGA measurement, 10 °C min^{-1} under N_2 atmosphere. [c] Determined from dynamic mechanical analysis. [d] Cross-link density at 80 °C calculated as $G_0 = 3\nu_e$ kT.

Characterization of PHU networks.

After recovery and post-curing, the PHUs were first characterized by FTIR spectroscopy (Figure SI-3 in Supporting Information). The presence of urethane moieties is evidenced by the absorption band at 1690 cm^{-1} and the complete conversion of carbonates is assumed as no remaining band at 1790 cm^{-1} is noticed.

The synthesized PHUs show comparable thermal stabilities (see TGA curves, Figure SI-4) and are all fully amorphous. Nevertheless, glass transition temperatures vary from 20 to 42 °C, significantly increasing with the amount of TAEA (Table 1, Figure SI-5). At first analysis, the Tg variation could be correlated to the number of H-bondings these networks can exhibit as a function of the TAEA/TMAEA ratio (Figure 2). Besides, the methyl moieties added in the case of secondary triamine incorporation (TMAEA) might increase the free volume in the network and, as a consequence decrease the energy necessary to the glass transition.

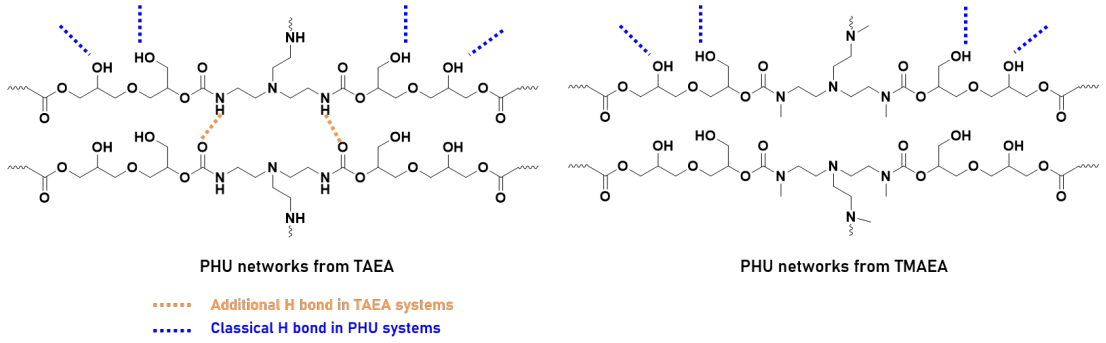

Figure 2. Additional H-bonds in networks synthesized from TAEA, compared to those synthesized with TMAEA.

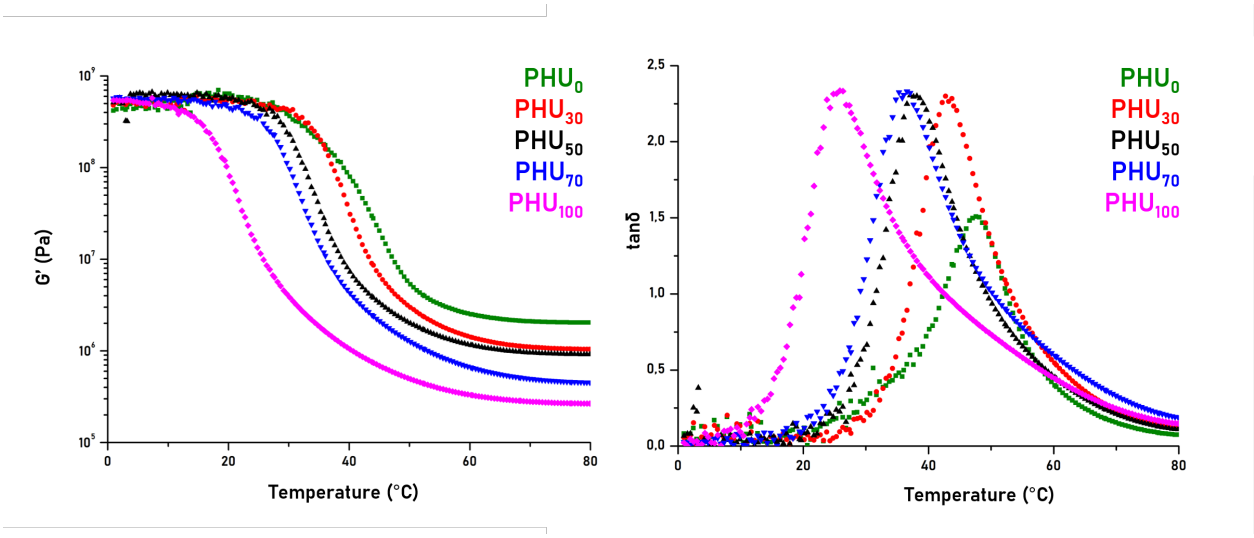

Figure 3. Evolution of storage shear modulus (left) and tan δ with temperature (1 Hz, 1000 Pa oscillatory stress) for PHU_0 (green), PHU_{30} (red), PHU_{50} (black), PHU_{70} (blue) and PHU_{100} (pink).

The cross-linked structure of the polymers was confirmed by swelling experiments in THF. Swelling ratios of 0 % for PHU_0, PHU_{30} and PHU_{50} even after 70 days and maximum swelling ratios of 4.6 % and 15 % after 70 days for PHU_{70} and PHU_{100} were measured, respectively. Gel contents were calculated, after 70 days in THF, between 89 % and 93.5 %. Detailed data are available in Table SI-2.

Dynamic mechanical analyses obtained from the first cooling ramp under 20 N compression, are displayed in Figure 3 and the corresponding characteristic values are reported in Table 1. The presence of elastic plateau (G_0) above T_g for all samples confirms that they are indeed chemically cross-linked, with a cross-link density (ν_e) considerably higher for samples with a higher amount of primary amines. This feature might be partially due to the additional H-bonds in PHU systems containing TAEA, leading to supplementary net-points in the networks. Also, the tan(δ) curves of samples with large amount of secondary amines (e.g. PHU_{70} and PHU_{100}) demonstrate significant asymmetry and tailing at high temperatures that are consistent with plausible network defects such as the presence of dangling chains. In contrast, the tan(δ) curve of PHU_0 rather displays shouldering around 30 °C, also visible as a two-step decay in the storage modulus, that could correspond to two distinct glass transitions in the sample. As of now, we do not have a proper explanation for this feature. The T_α values of all samples (measured at maxima of the loss moduli) are reported in Table 1 and demonstrate excellent accordance with T_g values. (Please note that standard DMA experiments are rather run using *heating* ramps that typically give higher T_α values).

Dual-Shape memory properties: Qualitative characterization

Dual-shape memory thermoresponsive behavior of the PHUs was first evidenced by visual experiments, as displayed in Figure 4. A strand of PHU_{30} (T_g = 34 °C) cured in a helical shape was deformed under heating ($T > T_g$) into a straight strand and immediately cooled at -20 °C during 15 min. The straight strand shape, stable at room temperature, is then heated a second time at 80 °C ($T > T_g$) and recovers its initial helical shape in a few seconds. This experience proves the dual shape memory ability of the DGDC-based PHUs and suggests that their thermoresponsive behavior is driven by the glass transition. Another example is displayed in Figure SI-6.

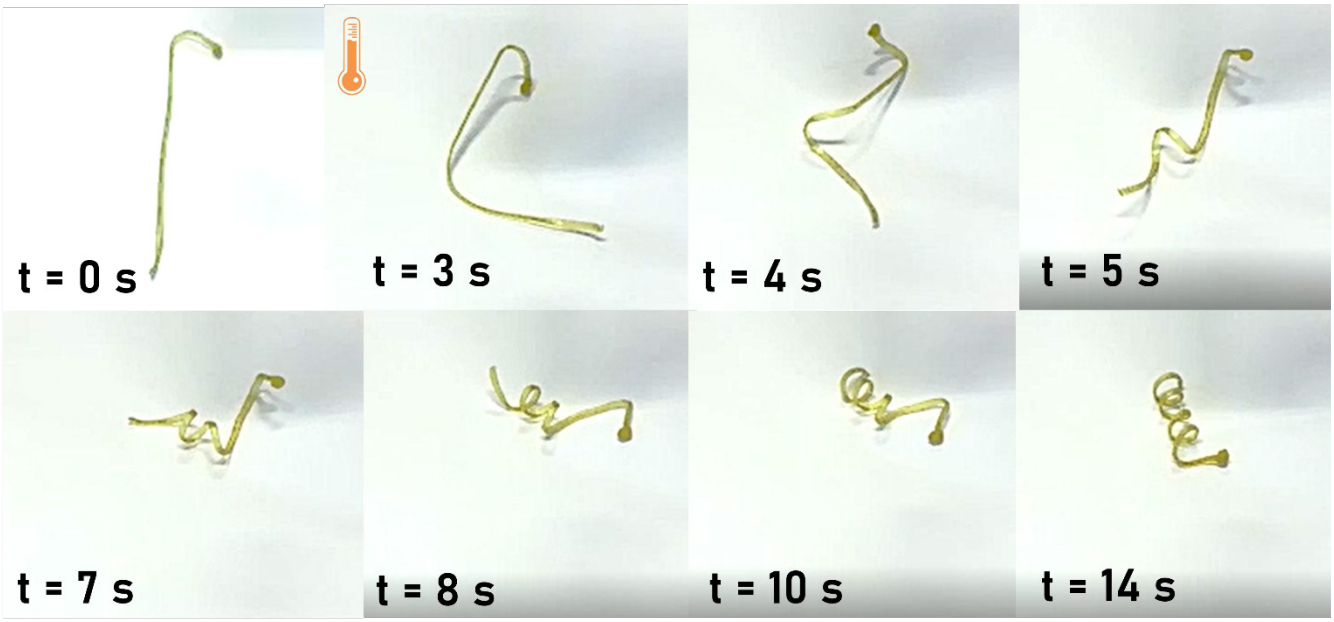

Figure 4. Shape memory behavior demonstration on PHU_{30}. A strand of PHU_{30} cured in a helical shape is deformed into a straight shape and cooled at -20 °C. Upon heating at 80 °C (heat gun) the initial shape is recovered in 14 seconds.

Dual-Shape memory properties: Quantitative characterization at 8o °C and effect of the TAEA/TMAEA ratio.

The shape memory properties of the PHUs were quantified by compressive fixation and recovery cycles as described in Figure 5.

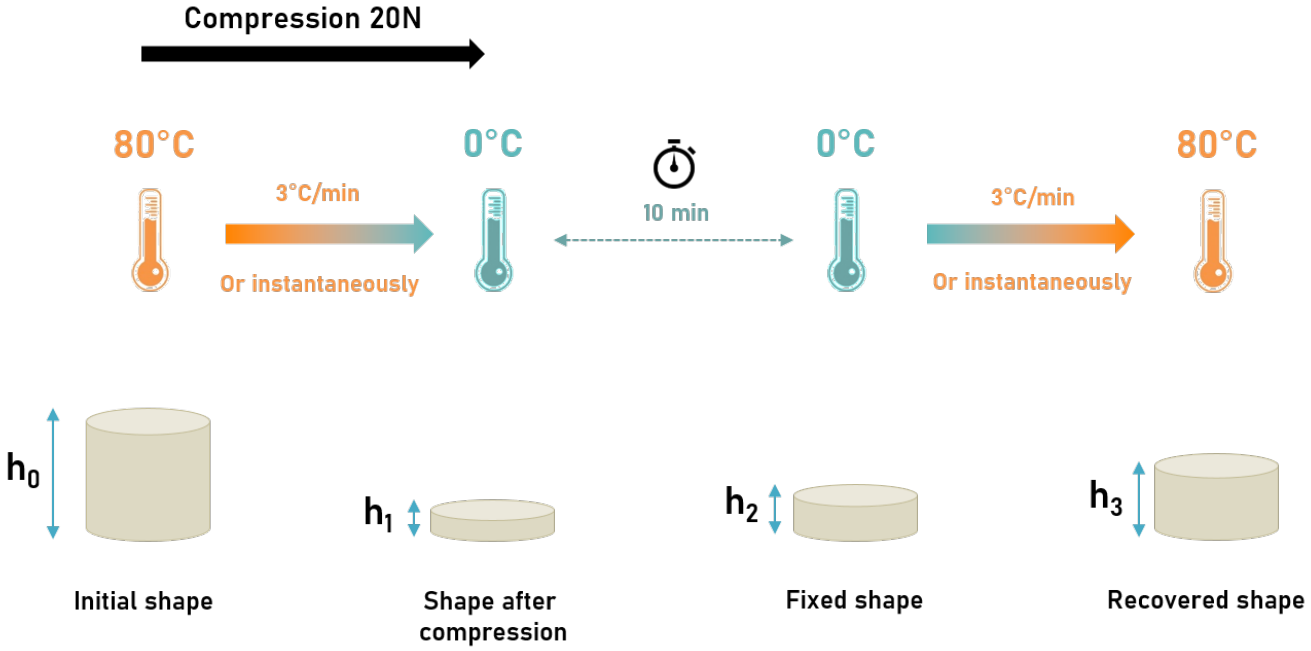

Figure 5. Shape memory property quantification protocol performed with rheometer.

A PHU disk (Figure 6) with initial height h_0, was placed at 80 °C and then compressed using a 20 N normal force while decreasing the temperature to 0 °C. The compressed height was labelled h_1. After release of normal force and 10 min equilibration at 0 °C, the fixed height, h_2, was measured. Finally, the sample is heated back at 80 °C and the recovered height, h_3 is measured. The different height values allow for the calculation of the recovery ratio (R_r) and the fixity ratio (R_f) (see calculation details in the experimental section). The cycle is repeated four times.

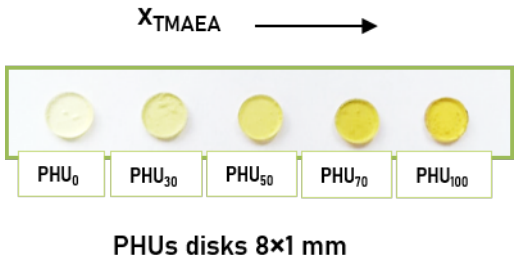

Figure 6. Cross-linked PHUs disks for rheometer characterization.

Figure 7 displays, as an example, PHU_0 height evolution recorded over time, in correlation with the normal force (F_N) and the temperature evolution. This graph proves the efficient height recovery of the PHU at 80 °C within the series of 4 cycles, as only the final height appears lower than the initial one.

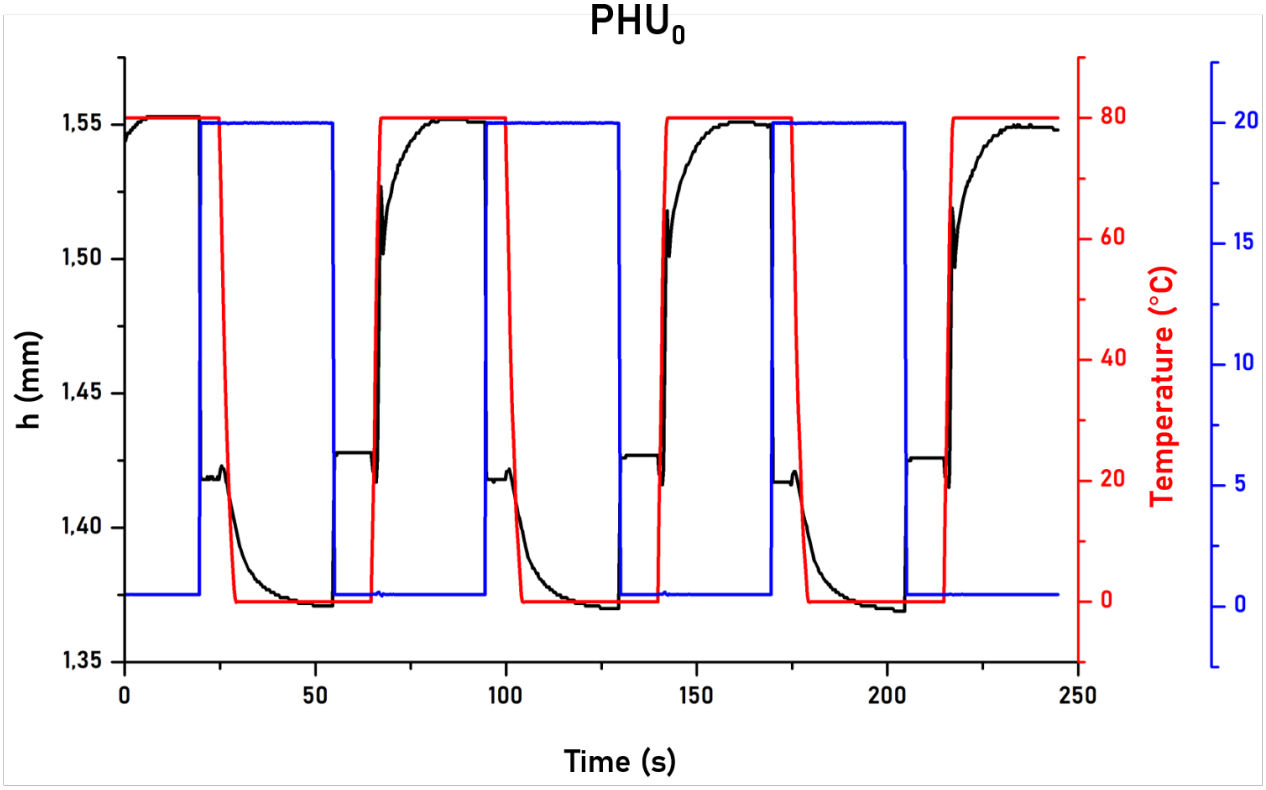

Figure 7. Thermoresponsive dual shape memory cycles 2, 3 and 4 of PHU_0 composed of h (black sample height), F_N (blue, normal force), and temperature (red). Data corresponding to $PHUs_{30-100}$ are available in SI, Figure SI-9.

Figure 8 display the variation of $(h(T) - h_1)/(h_0-h_1)$ as a function of temperature during the first fixing and recovery cycle of the PHUs. This representation enables direct visualization of the fixity ratio ($R_f = 1$ – ordinate immediately after unloading) and of the recovery ratio (R_r = ordinate after the end of the heating cycle). Height values have been corrected with thermal expansion (details in SI, Figures SI-7 et SI-8) in order to prove that the PHU T_g is effectively acting as the material T_{trans} and to verify that 80 °C is an appropriate temperature to perform the shape memory experiments (recovery complete and stable at 80 °C). Besides, sample height variations over temperature were normalized by compressive strains (h_0-h_1). For comparison, additional graphs representing heights sample variations only normalized by sample initial heights are available in SI, Figure SI-10. These values are reported for 4 successive cycles in Figure 9 and an excellent repeatability is demonstrated. The performances of the shape memory PHUs are not significantly altered over a few cycles. While PHU_{0-70} demonstrated excellent recovery from 92 to 98%, the recovery ratio value was significantly reduced for PHU_{100}. These results are consistent with the dynamic mechanical analyses pointing towards defects in this network. Such heterogeneities enable indeed to relax partially the fixation-induced stresses and consequently limit the full recovery of the initial shape. In contrast, the R_f values are increasing with the content of secondary amines. We believe this to be directly related to the significant decrease of the cross-link density of PHU networks. The recovery onset temperatures, indicated by arrows on the graph, are very close to the T_α transitions previously reported, which confirms that the shape memory behavior is indeed governed by the glass transition. Interestingly, the unexpected dual transition previously detected in PHU_0 has a considerable influence on the recovery, as the onset starts as early as 32 °C, which corresponds to the first relaxation observed in tan(δ) on Figure 3.

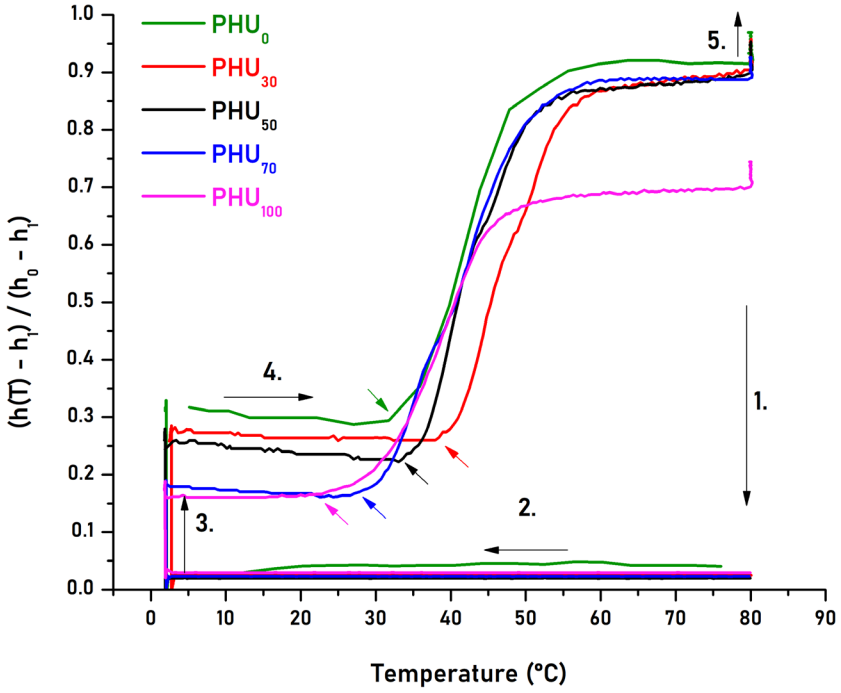

Figure 8. Variation of disk height during the first fixing and recovery steps of PHUs with temperature ramps of 3 °C min^{-1}. 1. Compression, 2. Cooling while maintaining the compression, 3. Unloading, 4. Heating, 5. Equilibration at 80 °C for 20 min. Height values have been corrected with thermal expansion.

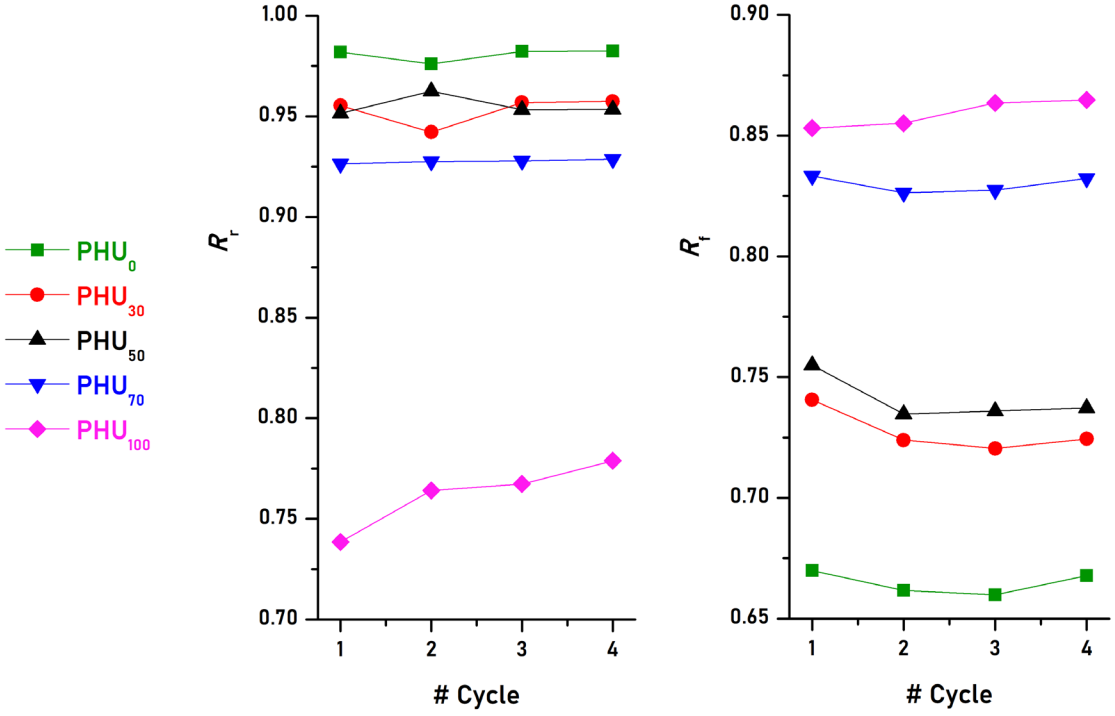

Figure 9. Shape Recovery and Fixity ratios calculated from equations 1 and 2 (See materials and methods) during 4 cycles for PHUs$_{0\text{-}100}$.

Dual-Shape memory properties: Quantitative characterization at 37 °C and effect of the TAEA/TMAEA ratio.

As materials exhibiting shape memory properties are of great interest for biomedical applications, DGDC-based PHUs recovery properties were tested at body temperature (37 °C). After compression (normal force = 20 N) and cooling at 0 °C, the samples were unloaded and the temperature was instantaneously increased to 37 °C to monitor shape recovery during 2 hours. The corresponding $R_{r,37°C}(t)$ rates are displayed in Figure 10.

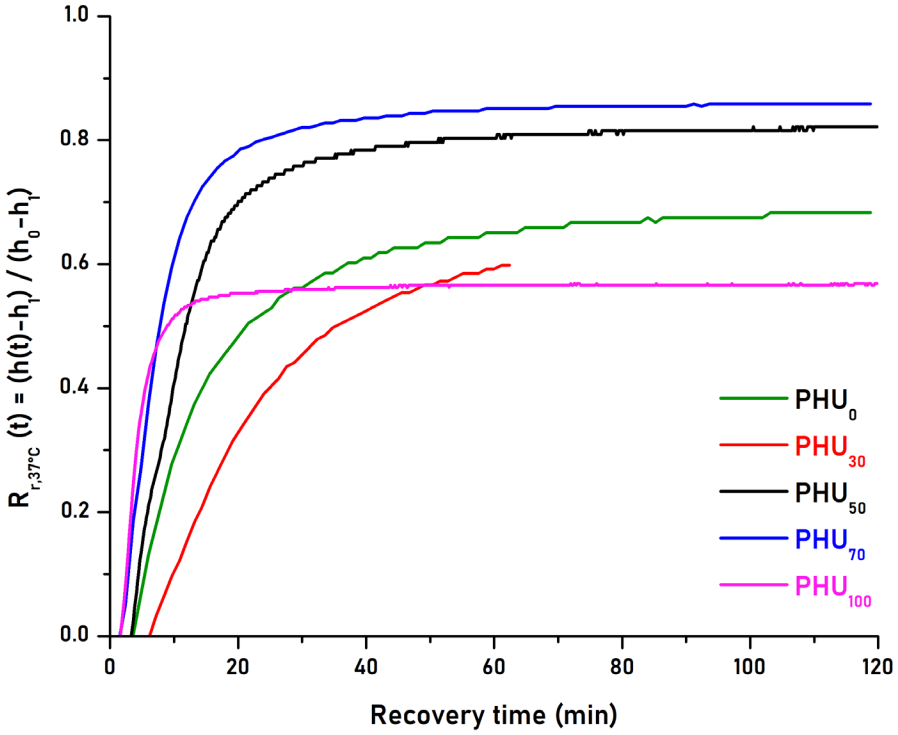

Figure 10. Recovery ratio over time at 37 °C for PHU_0 (green), PHU_{30} (red), PHU_{50} (black), PHU_{70} (blue) and PHU_{100} (pink).

Two distinctive features can be observed during these recovery experiments. On the one hand, the initial slope is characteristic of the mobility in these networks at 37 °C and increases as the T_α of the networks decrease (curves fitting were performed in order to determine relaxation times associated to each PHU system, see supporting information, Table SI.3). We also find in these experiments that initial recovery of PHU_0 is faster than the one of PHU_{30} and governed by the first relaxation. On the other hand, the asymptotic recovery is linked to the maximal recovery ratio at 80 °C and related to the distribution of the relaxation temperatures: while PHU_0 and PHU_{30} previously demonstrated the highest maximal recoveries, a high fraction of the overall tan(δ) is shifted above 37 °C and, consequently, a large part of their relaxation remains frozen at 37 °C. PHU_{50} and PHU_{70} show in the present situation the best compromises between high maximal recoveries and sufficiently low T_α values, with $R_{r,37\,°C}$ values above 80 %, and these two materials are therefore the most promising for potential biomedical applications.

Hydrodegradation of DGDC-based cross-linked PHUs

PHU systems are known to show exacerbated hydrophily and water absorption, comparatively to PU analogous due to the hydroxyl moieties on their backbone.[4] DGDC-based PHUs were here tested regarding their stability towards air humidity and water immersion.
$PHUs_{0\text{-}100}$ were first tested regarding their stability toward ambient air moisture. After 30 days in open-air, the DSC first heating cycle of the PHU samples (grey curves on the graphs on Figure 11 (a) show a drastic drop in polymer T_gs. For instance, after 30 days in open-air, the T_g of PHU_{100}, initially equal to 20 °C, drops to -13 °C. PHU water absorption is responsible of this plasticization phenomenon, as already reported for some PU systems.[26] Besides, after drying at 30 °C under vacuum, T_g values can be increased (green curves). Finally, the drying at 80 °C allowed the recovery of the initial T_g values, proving the reversibility of this phenomenon and the absence of related chemical degradation. Overlays of DSC curves for $PHUs_{30\text{-}100}$ are available in supporting information (Figure SI-11)

In addition, the ability of PHU_0 and PHU_{100} to absorb water was quantified by a 48 h analysis at 80 °C by mean of TGA; the corresponding weight losses curves are displayed in Figure 11 (b). Final weight losses of 5.9 % and 4.9 % were calculated for PHU_{100} and PHU_0 respectively. According to the temperature set for the analysis, these losses can undoubtedly be assigned to water evaporation.

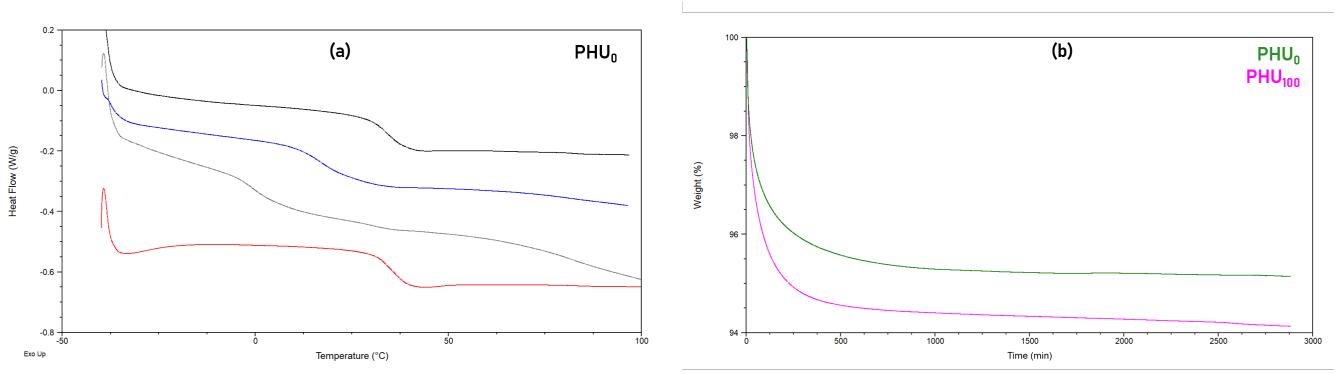

Figure 11. DSC first heating cycles of PHU_0 (a), initial sample (black curve), sample after 30 days in the open-air (grey), sample dried at 30 °C under vacuum (blue curve), and sample after 48 h drying at 80 °C (red) (a). TGA traces obtained for PHU_0 (green curve) and PHU_{100} (pink curve) during 48 h isothermal analysis at 80 °C (b). Additional data available in Figure SI-11.

Regarding the previous results in terms of water uptake, the stability of the networks in water was investigated. Rectangular pieces of the 5 PHUs were introduced in closed flasks containing D_2O and let at room temperature (see Figure 12). After a first swelling stage, the materials were fully dissolved in water after few months. By the meantime, the pH of the water solution was measured close to 10, suspecting a degradation of the networks by hydrolysis (Figure SI-12).

Figure 12. Water stability test of DGDC-based PHUs.

Indeed, urethane moieties are subject to water nucleophilic attack, leading to a carbamic acid and an alcohol, followed by a decarboxylation step, releasing an amine and CO_2. Finally, in the presence of CO_2, amines can be carbonated, producing ammonium salt and sodium bicarbonate (Figure 13). Nevertheless, one may suspect the presence of moisture sensitive urea bonds in PHUs materials, that would be responsible for the observe hydrolysis. Despite the absence of bands correspond urea linkage on the FTIR spectra, additional HR-MAS analysis was performed on PHU0, in order to confirm the absence of this common by-product in PHU synthesis (Supporting information Figure SI-13).

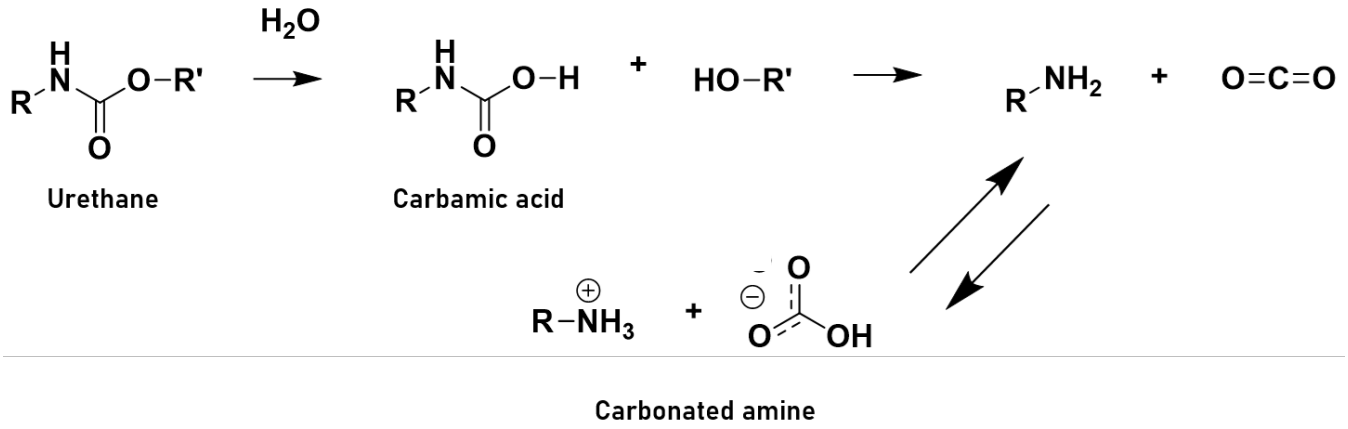

Figure 13. Mechanism of urethane moieties hydrolysis, leading first to carbamic acid, and then to an amine after decarboxylation. The so-created amine is then subjected to carbonation with the CO_2 generated in-situ.

In order to prove this phenomenon and the proposed mechanism, hydrolysates, (solution of the dissolved PHUs in D_2O, labelled Hyd-PHU_x), were analyzed and, as an example, Hyd-PHU_{30} was freeze-dried and the resulting product was analyzed by FTIR, SEC in DMF and ^1H NMR in DMSO-d_6.

SEC traces obtained in DMF (Figure SI-14, right) shows very low molar masses, (calculated according to PS standards) proving the exclusive presence of fragments in Hyd-PHU$_{30}$. Besides, the FTIR spectrum shows a new absorption band around 2500 cm^{-1}, compared to the spectrum of the initial PHU$_{30}$ (not hydrolyzed) (Figure SI-14, left). This band might be attributed to COOH and/or NH_3^+ functions, which is consistent with the proposed hydrolysis mechanism. Finally, in order to identify the possible fragments present in PHU hydrolysates, an hydroxyurethane model compound (HU-m) was synthesized from DGDC and hexylamine. The comparison between the NMR spectrum of Hyd-PHU$_{30}$ after freeze drying and HU-m in DMSO-d6 (Figure 14) confirms their similar structure and prove the very low resulting amount of urethane functions after hydrolysis.

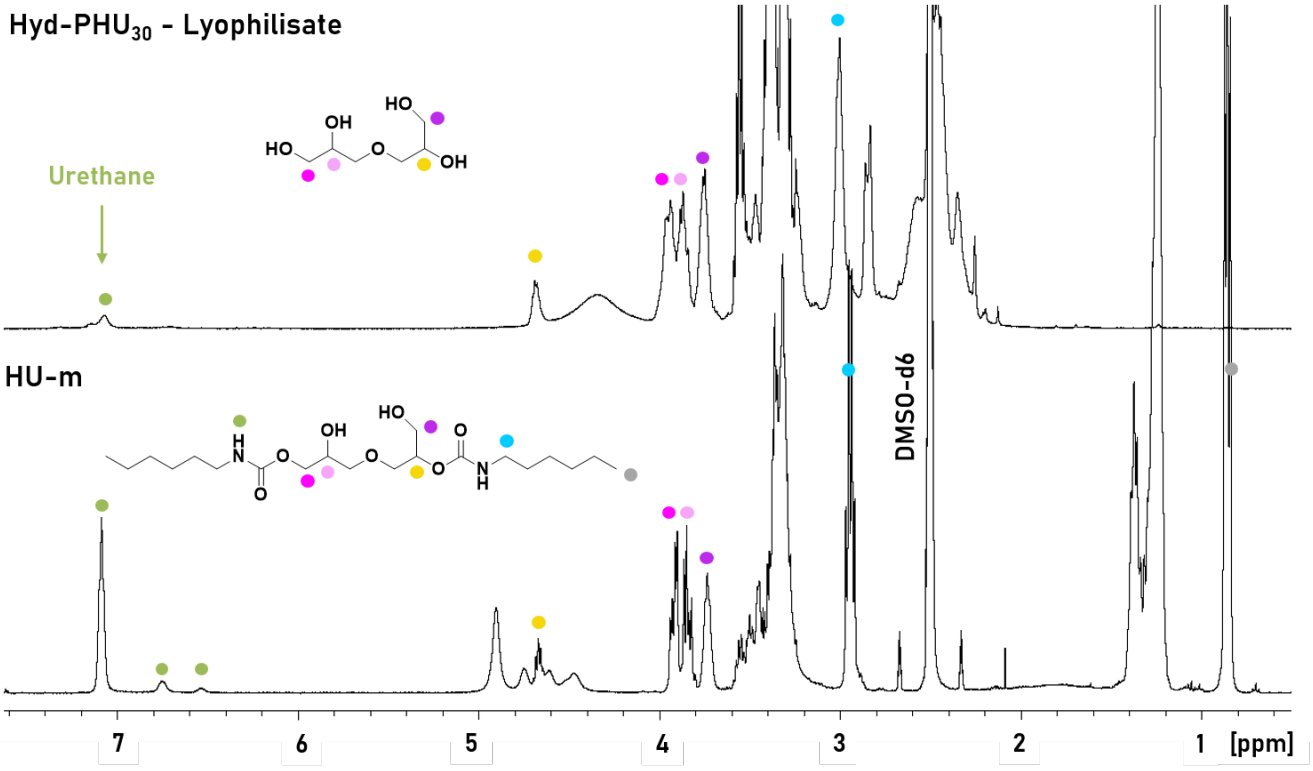

Figure 14. Stacked ^{1}H NMR spectra of Hyd-PHU$_{30}$ lyophilisate (top), compared to HU-m model compound (bottom), in DMSO-d6 at 25 °C.

Simultaneously, Hyd-PHUs$_{0\text{-}100}$ in D_2O were directly analyzed by ^{1}H NMR (Figure 15). The stacked ^{1}H NMR spectra show that the signals between 3.5 and 4.3 ppm are similar for each PHU hydrolysate, whereas the signals in the area between 2.5 and 3.5 ppm are different according to the TAEA/TMAEA ratio. The signals in the last area can be assigned to protons belonging to the amine functions and their carbonated forms. In order to identify the signals corresponding to the carbonated amine, model carbonation was performed on TAEA and TMAEA. The amines were solubilized in D_2O and ^{1}H NMR analyses were performed before and after CO_2 flushing (30 minutes) directly into the NMR tube. The resulting spectra were compared clearly demonstrating the formation of carbonated amines with the appearance of new signals at 3.25, 3.07, 2.82, 2.79, 2.69 and 2.67 ppm for TMAEA and 3.09, 2.84, 2.60 ppm for TAEA. (Figure 16)

Finally, the ^{1}H NMR spectrum of HU-m model compound recorded in D_2O was compared to the ones of the Hyd-PHU$_0$ and Hyd-PHU$_{100}$, and carbonated amines (Figure 17). As can be seen, the presence of carbonated amine in the hydrolysates is clearly identifiable. Besides, the comparison with HU-m confirms that the fraction of the polymeric material containing the ester moiety stays intact and is not subject by hydrolysis.

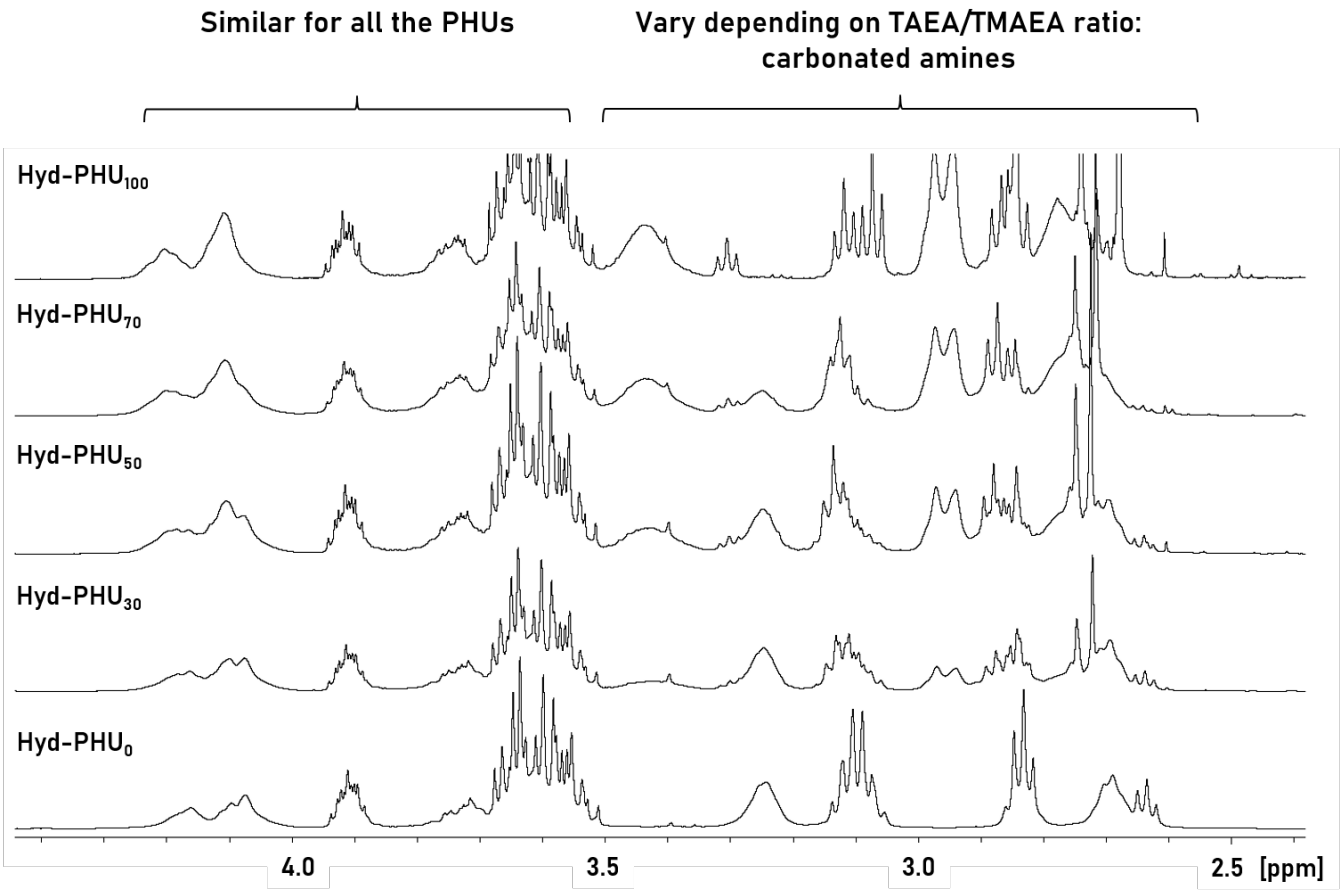

Figure 15. Stacked NMR spectra in D2O, at 25 °C, of Hyd-PHUs$_{0\text{-}100}$. Zoom between 2.4 and 4.4 ppm.

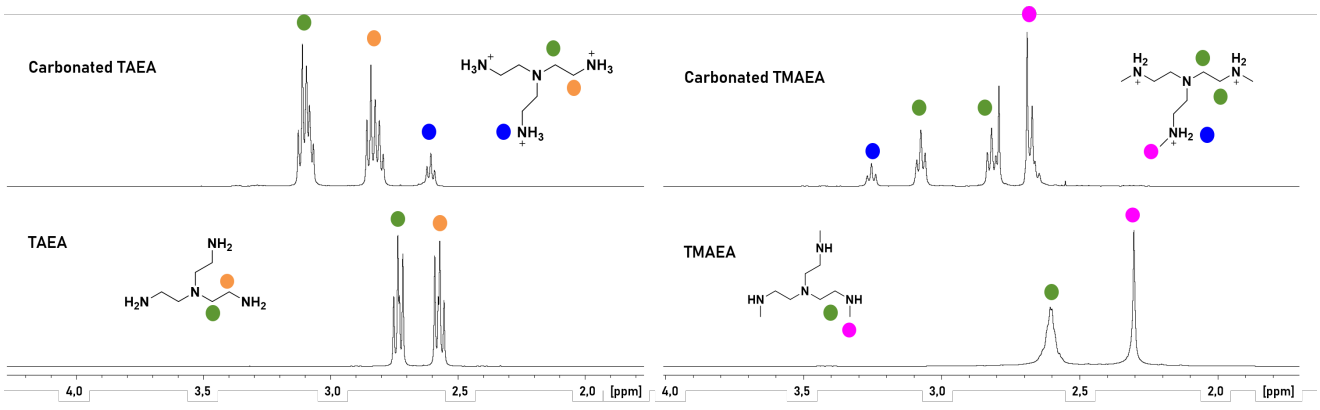

Figure 16. Stacked NMR spectra in D_2O, 25 °C of TAEA (bottom, left), TMAEA (bottom right) and of their respective carbonated forms (up).

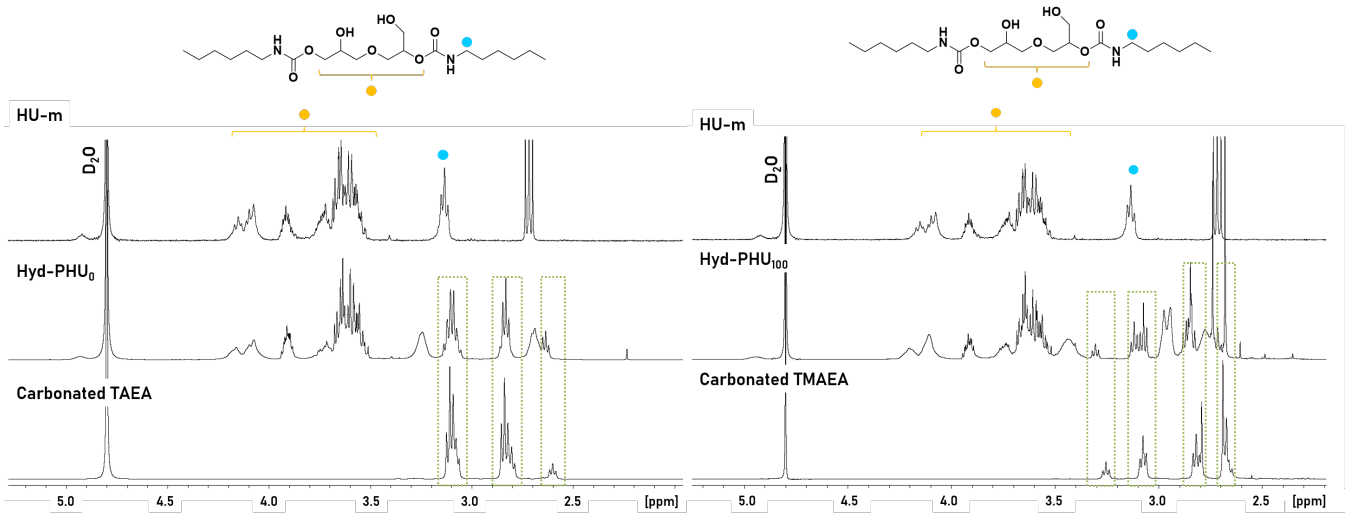

Figure 17. Stacked ^{1}H NMR spectra of carbonated TAEA and TMAEA (bottom), Hyd-PHU$_0$ and Hyd-PHU$_{100}$ (middle), and a model compound HU-m (top), in D_2O at 25 °C.

CONCLUSION

A series of DGDC-based PHUs networks have been synthesized by reactive extrusion in short reaction and curing times. These materials exhibit shape memory properties, triggered by heat. In the case of these cross-linked amorphous materials, the T_g plays the role of T_{trans} and the chemical cross-links acts as netpoints in the matrix. Dual-shape memory ability was first investigated at 80°C, a temperature sufficiently higher than the polymer T_gs. The final average recovery ratios calculated are very close to 100 % for most of the PHUs. Besides, as numerous SMPs find application in the biomedical field, the shape memory ability was tested at 37 °C. Recovery ratios up to 86 % were calculated. Besides, the recovery kinetic of these DGDC-based cross-linked PHU systems is tunable by the TAEA/TMAEA ratio.
Finally, the DGDC-based PHU networks show ability to be degraded through hydrolysis in relatively short times (few months), depending on the amount of TMAEA incorporated in the polymer matrix. This last feature is undoubtedly interesting and should be valorized for some applications and in particular in the biomedical field.

ASSOCIATED CONTENT

Supporting Information

The supporting information contains additional scheme explaining shape memory principle, details on the curing procedure and shape memory characterization protocol, FTIR spectra, TGA traces, DSC second heating cycles and swelling ratios in THF of PHUs$_{0\text{-}100}$, illustration on another visual example of PHU shape recovery capacity, thermal expansion correction applied to recovery curves, additional data about shape recovery thermomechanical quantification, overlay of DSC first heating cycles before and after ambient air moisture exposition, illustration of pH measurement, HR-MAS spectrum, SEC and FTIR analysis on lyophilized PHU.

AUTHOR INFORMATION

Corresponding author

cramail@enscbp.fr
egrau@enscbp.fr
damien.montarnal@univ-lyon1.fr

Note

The authors declare no competing financial interest.

ACKNOWLEDGEMENTS

The authors gratefully acknowledge the financial support from Region Nouvelle Aquitaine and ITERG (French Institute for Fats and Oils)

REFERENCES

(1) Nohra, B.; Candy, L.; Guerin, C.; Raoul, Y. From Petrochemical Polyurethanes to Biobased Polyhydroxyurethanes. **2013**, *46* (10), 3771–3792.

(2) Schmidt, S.; Göppert, N. E.; Bruchmann, B.; Mülhaupt, R. Liquid Sorbitol Ether Carbonate as Intermediate for Rigid and Segmented Non-Isocyanate Polyhydroxyurethane Thermosets. *Eur. Polym. J.* **2017**, *94*, 136–142.

(3) Blattmann, H.; Mülhaupt, R. Multifunctional POSS Cyclic Carbonates and Non-Isocyanate Polyhydroxyurethane Hybrid Materials. *Macromolecules* **2016**, *49* (3), 742–751.

(4) Schimpf, V.; Heck, B.; Reiter, G.; Mülhaupt, R. Triple-Shape Memory Materials via Thermoresponsive Behavior of Nanocrystalline Non-Isocyanate Polyhydroxyurethanes. *Macromolecules* **2017**, *50* (9), 3598–3606.

(5) Schimpf, V.; Asmacher, A.; Fuchs, A.; Bruchmann, B.; Mülhaupt, R. Polyfunctional Acrylic Nn-Isocyanate Hydroxyurethanes as Photocurable Thermosets for 3D Printing. *Macromolecules* **2019**, *52* (9), 3288–3297.

(6) Gennen, S.; Grignard, B.; Thomassin, J. M.; Gilbert, B.; Vertruyen, B.; Jerome, C.; Detrembleur, C. Polyhydroxyurethane Hydrogels: Synthesis and Characterizations. *Eur. Polym. J.* **2016**, *84*, 849–862.

(7) Magliozzi, F.; Chollet, G.; Grau, E.; Cramail, H. Benefit of the Reactive Extrusion in the Course of Polyhydroxyurethanes Synthesis by Aminolysis of Cyclic Carbonates. *ACS Sustain. Chem. Eng.* **2019**, *7* (20), 17282–17292.

(8) Pilate, F.; Toncheva, A.; Dubois, P.; Raquez, J. M. Shape-Memory Polymers for Multiple Applications in the Materials World. *Eur. Polym. J.* **2016**, *80*, 268–294.

(9) Hubbard, A. M.; Luong, E.; Ratanaphruks, A.; Mailen, R. W.; Genzer, J.; Dickey, M. D. Shrink Films Get a Grip. *ACS Appl. Polym. Mater.* **2019**, *1* (5), 1088–1095.

(10) Santo, L.; Quadrini, F.; Accettura, A.; Villadei, W. Shape Memory Composites for Self-Deployable Structures in Aerospace Applications. *Procedia Eng.* **2014**, *88*, 42–47.

(11) Liu, Y.; Du, H.; Liu, L.; Leng, J. Shape Memory Polymers and Their Composites in Aerospace Applications: A Review. *Smart Mater. Struct.* **2014**, *23* (2).

(12) Gök, M. O.; Bilir, M. Z.; Gürcüm, B. H. Shape-Memory Applications in Textile Design. *Procedia - Soc. Behav. Sci.* **2015**, *195*, 2160–2169.

(13) Hu, J.; Meng, H.; Li, G.; Ibekwe, S. I. A Review of Stimuli-Responsive Polymers for Smart Textile Applications. *Smart Mater. Struct.* **2012**, *21* (5).

(14) Lu, H.; Yu, K.; Liu, Y.; Leng, J. Sensing and Actuating Capabilities of a Shape Memory Polymer Composite Integrated with Hybrid Filler. *Smart Mater. Struct.* **2010**, *19* (6).

(15) Ware, T.; Simon, D.; Hearon, K.; Liu, C.; Shah, S.; Reeder, J.; Khodaparast, N.; Kilgard, M. P.; Maitland, D. J.; Rennaker, R. L.; et al. Three-Dimensional Flexible Electronics Enabled by Shape Memory Polymer Substrates for Responsive Neural Interfaces. *Macromol. Mater. Eng.* **2012**, *297* (12), 1193–1202.

(16) Small, W.; Singhal, P.; Wilson, T. S.; Maitland, D. J. Biomedical Applications of Thermally Activated Shape Memory Polymers. *J. Mater. Chem.* **2010**, *20* (17), 3356–3366.

(17) Lendlein, A. Shape-memory Polymers. *Angew. Chemie Int.* **2002**, *41*, 2034–2057.

(18) Conjugated, T. M.; Langer, R. Light-Induced Shape-Memory Polymers ¨. **2005**, *434* (April), 695–697.

(19) Razzaq, M. Y.; Anhalt, M.; Frormann, L.; Weidenfeller, B. Thermal, Electrical and Magnetic Studies of Magnetite Filled Polyurethane Shape Memory Polymers. *Mater. Sci. Eng. A* **2007**, *444* (1–2), 227–235.

(20) Bossion, A.; Aguirresarobe, R. H.; Irusta, L.; Taton, D.; Cramail, H.; Grau, E.; Mecerreyes, D.; Su, C.; Liu, G.; Müller, A. J.; et al. Unexpected Synthesis of Segmented Poly(Hydroxyurea-Urethane)s from Dicyclic Carbonates and Diamines by Organocatalysis. *Macromolecules* **2018**, *51* (15), 5556–5566.

(21) Van Velthoven, J. L. J.; Gootjes, L.; Van Es, D. S.; Noordover, B. A. J.; Meuldijk, J. Poly(Hydroxy Urethane)s Based on Renewable Diglycerol Dicarbonate. *Eur. Polym. J.* **2015**, *70*, 125–135.

(22) Tryznowski, M.; Świderska, A.; Zołek-Tryznowska, Z.; Gołofit, T.; Parzuchowski, P. G. Facile Route to Multigram Synthesis of Environmentally Friendly Non-Isocyanate Polyurethanes. *Polymer (Guildf).* **2015**, *80*, 228–236.

(23) Schimpf, V.; Max, J. B.; Stolz, B.; Heck, B.; Mülhaupt, R. Semicrystalline Non-Isocyanate Polyhydroxyurethanes as Thermoplastics and Thermoplastic Elastomers and Their Use in 3D Printing by Fused Filament Fabrication. *Macromolecules* **2019**, *52* (1), 320–331.

(24) Khedaioui, D.; Boisson, C.; D'Agosto, F.; Montarnal, D. Polyethylene Aerogels with Combined Physical and Chemical Crosslinking: Improved Mechanical Resilience and Shape-Memory Properties. *Angew. Chemie - Int. Ed.* **2019**, *58* (44), 15883–15889.

(25) Camara, F.; Benyahya, S.; Besse, V.; Boutevin, G.; Auvergne, R.; Boutevin, B.; Caillol, S. Reactivity of Secondary Amines for the Synthesis of Non-Isocyanate Polyurethanes. *Eur. Polym. J.* **2014**, *55*, 17–26.

(26) Garces, I. T.; Aslanzadeh, S.; Boluk, Y.; Ayranci, C. Effect of Moisture on Shape Memory Polyurethane Polymers for Extrusion-Based Additive Manufacturing. *Materials (Basel).* **2019**, *12* (2).

SUPPORTING INFORMATION

Hydrolysable bio-based polyhydroxyurethane networks with shape memory behavior at body temperature

Fiona Magliozzi[1], Arthur Scali[1], Guillaume Chollet[3], Damien Montarnal[2*], Etienne Grau[1*], Henri Cramail[1*]

[1]Univ. Bordeaux, CNRS, Bordeaux INP, LCPO, UMR 5629, F-33600, Pessac, France

[2]Univ Lyon, Université Claude Bernard Lyon 1, CPE Lyon, CNRS, UMR 5265, C2P2, 43 Bvd. du 11 Novembre 1918, F-69616 Villeurbanne, France

[3]ITERG, 11 rue Gaspard Monge, 33610 Canéjan, France

Pages: 15

Figures: 14

Tables: 3

I. Introduction

II. Experimental section

III. Thermosets materials characterization

IV. Shape memory and recovery quantification

V. PHU hydrolysis

I. Introduction

Most of shape memory polymers (SMPs) are dual-shape memory polymers (dual-SMPs), capable of memorizing two different shapes: a permanent shape (shape B) given by the manufacturing process and a temporary shape (shape A), given by a mechanical deformation under specific conditions (programming). Materials capable of shape recovery can actively change from shape B to shape A, when an external stimulus is applied.

Shape memory property only relies on the molecular architecture of the polymer and no specific moieties or repeating units are needed. Nevertheless, a three dimensional structure is mandatory, whether it is composed of chemical or physical cross-links. SMPs are this way compared to elastic polymer network equipped with stimuli-sensitive switches and netpoints (Figure SI.1). While the netpoints determine the permanent shape of the network, the switches are the flexible parameters enabling to induce or restrict the chain mobility in the polymer matrix.

External stimuli such as light, magnetic or electric fields can be used, but the most common is heat, leading to thermoresponsive shape memory behavior. In this case, the shape recovery is driven by a specific transition temperature called T_{trans}. When $T>T_{trans}$ the switching domains are flexible, releasing the entropy stored and resulting in an elastic entropic behavior of the polymer above T_{trans}.

For SMPs, T_{trans} can be the T_g, specifically in the case of chemically cross-linked systems, or T_m, if the network is generated by physical cross-links (crystalline domains).

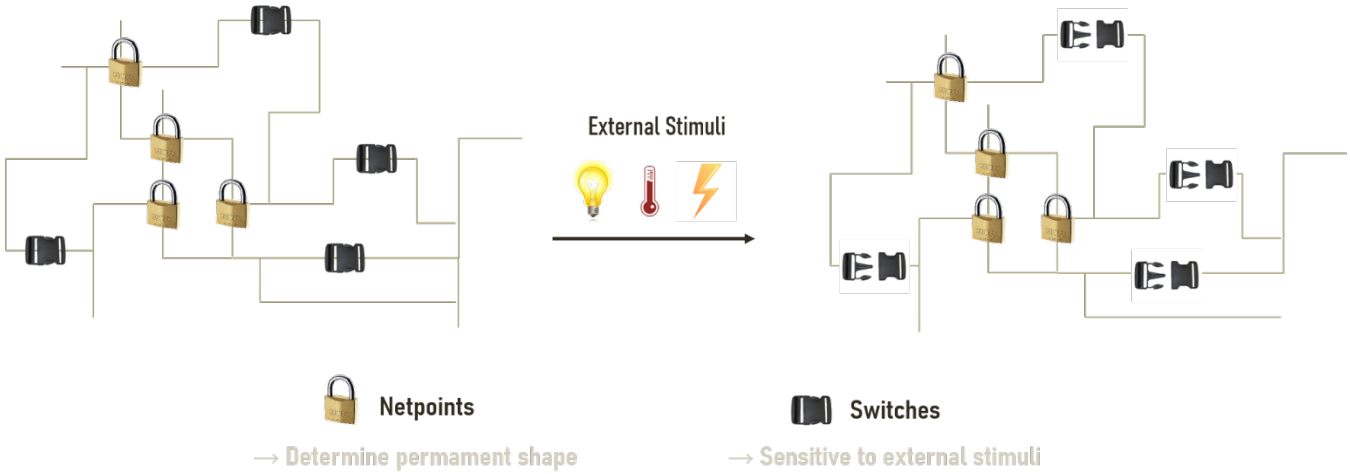

Figure SI.1. Shape memory effect relying on molecular architecture: netpoints (padlocks) and molecular switches (clip lock).

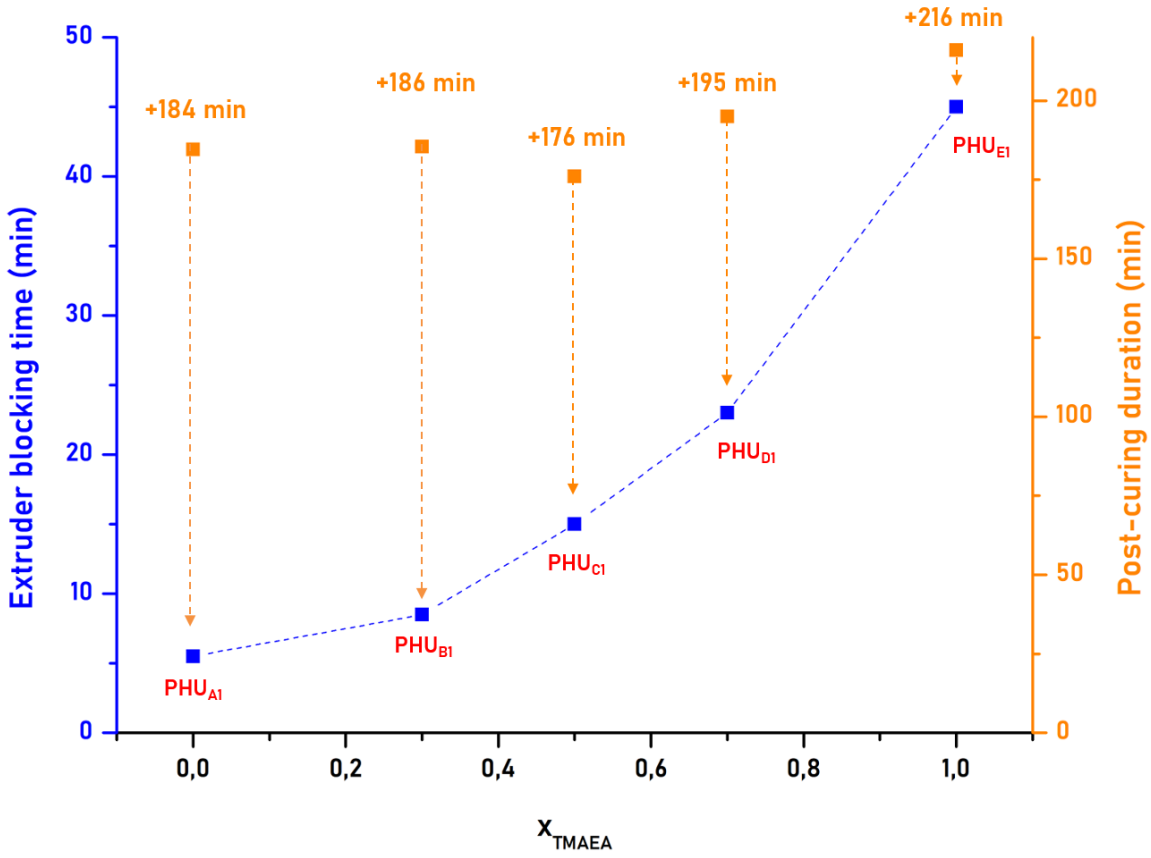

Figure SI-2. Extruder blocking times and adapted post-curing times depending on the TMAEA/TAEA ratio.

Table SI.1. Shape memory rheometry characterization protocol and parameters applied for the different steps.

Step		Step Name	$T_{initial}$ (°C)	T_{final} (°C)	Duration (min)	F_N (N)	Rate
1		Isothermal	0		20	0.5	
		Expansion	0	80	27	0.5	3 °C/min
2		Isothermal	80		5	0.5	
		Isothermal Compression	80		5	20	
		Temperature decreased + modulus measurement	80	0	27	20	3 °C/min
		Isothermal compressed cold	0		5	20	
		Isothermal released cold	0		10	0.5	
		Temp increase : T_{trans} determination	0	80	27	0.5	3 °C/min
3	CY_0	Isothermal released hot	80		20	0.5	
	CY_1	Isothermal compressed hot	80		5	20	
		Isothermal compressed cold	0		30	20	
		Isothermal released cold	0		10	0.5	
		Isothermal released hot	80		30	0.5	
	CY_2	Isothermal compressed hot	80		5	20	
		Isothermal compressed cold	0		30	20	
		Isothermal released cold	0		10	0.5	
		Isothermal released hot	80		30	0.5	
	CY_3	Isothermal compressed hot	80		5	20	
		Instant	0		30	20	
		Isothermal released	0		10	0.5	
		Instant	80		30	0.5	
4		Modulus measurement	80		5	0,5	
		Isothermal released hot	80		20	0.5	
		Isothermal compressed hot	80		5	20	
		Isothermal compressed cold	0		30	20	
		Isothermal released cold	0		10	0.5	
		Isothermal released 37°C	37		120	0.5	
5	F_{20}	Isothermal released hot	80		5	0.5	
		Isothermal compression hot	80		5	20	
		Isothermal compression cold	20		30	20	
		Isothermal released cold	20		60	0.5	
	F_4	Isothermal released hot	80		5	0.5	
		isothermal compression hot	80		5	20	
		Isothermal compression cold	4		30	20	
		Isothermal released cold	4		60	0.5	
	M	Modulus measurement	80		10	0.5	

*No heating rate mentioned = temperature changed instantaneously

II. Thermosets characterization

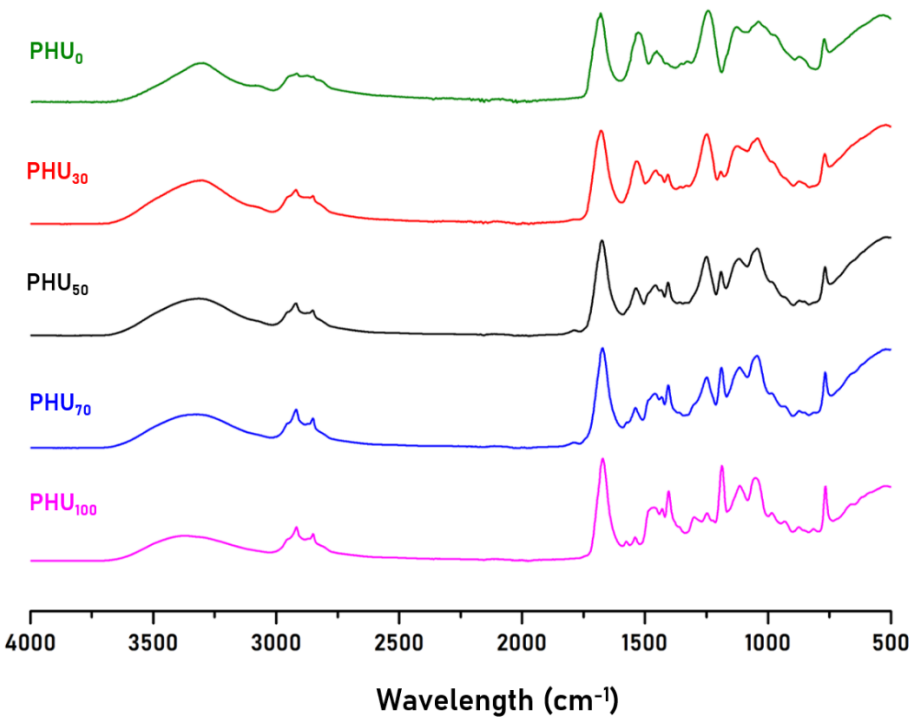

Figure SI-3. FTIR spectra of PHU_0 (green), PHU_{30} (red), PHU_{50} (black), PHU_{70} (blue) and PHU_{100} (pink).

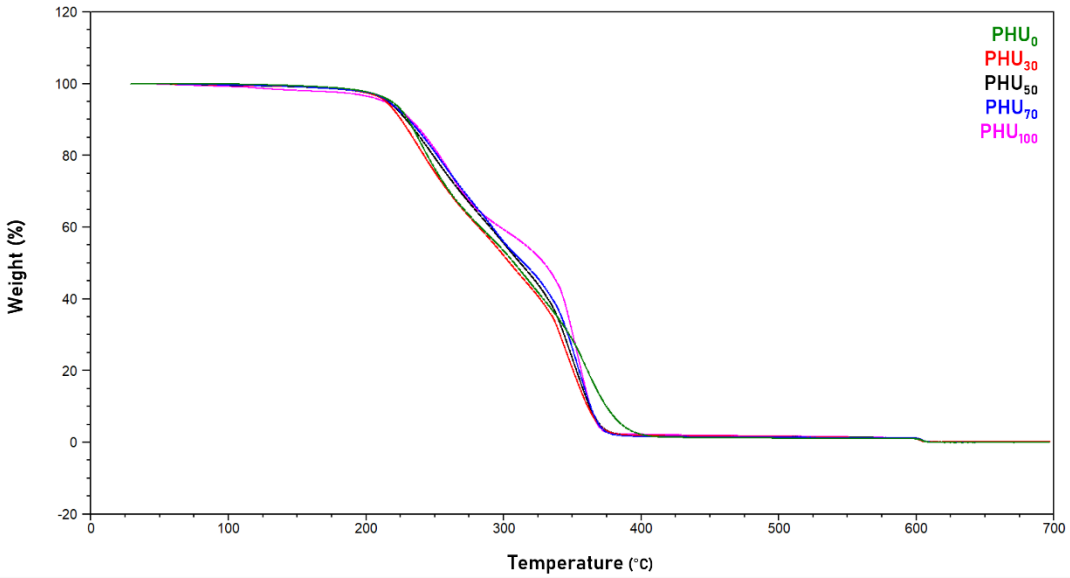

Figure SI-4. Overlay of TGA traces of $PHUs_{0\text{-}100}$ measured by TGA.

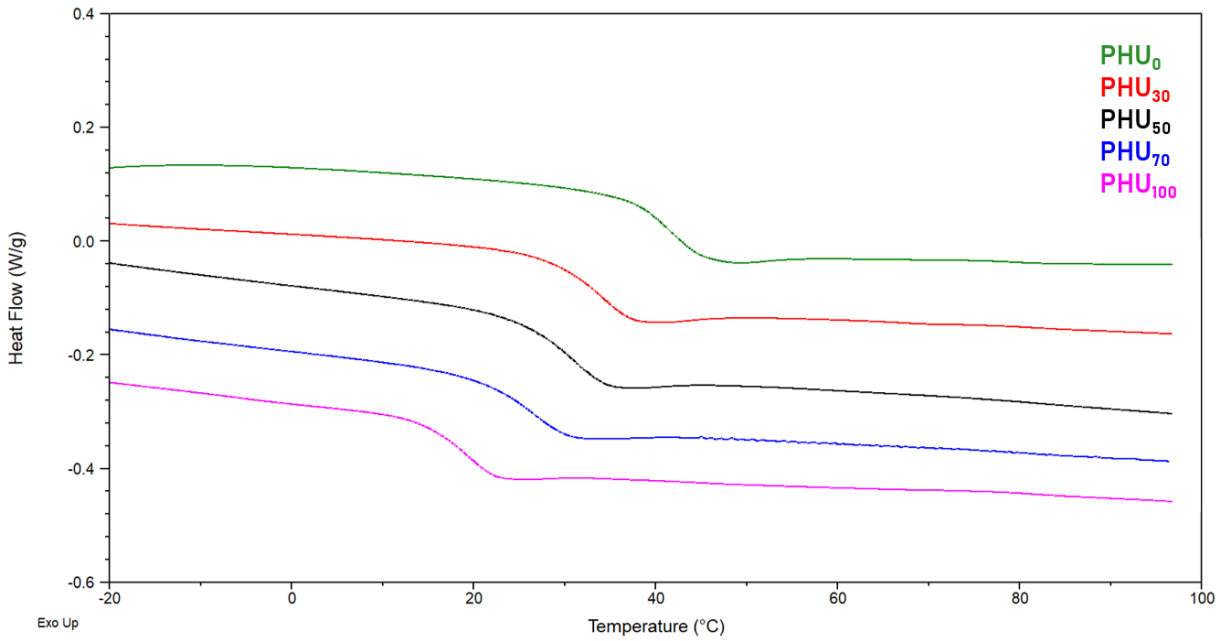

Figure SI-5. Overlay of DSC second heating cycles of PHU_0 (green), PHU_{30} (red), PHU_{50} (black), PHU_{70} (blue) and PHU_{100} (pink).

Table SI-2. Swelling ratios and gel contents in THF for $PHUs_{0\text{-}100}$ from 1 to 70 days.

	Swelling ratios (%)				Gel content (%)
Time	**1 days**	**2 days**	**24 days**	**70 days**	**70 days**
PHU_0	0	0	0	0	93,5
PHU_{30}	0	0	0	0	93,3
PHU_{50}	0	0	0	0	93,3
PHU_{70}	0,20	0,70	1,40	4,63	91,1
PHU_{100}	3,08	6,29	16,7	15,4	89,1

III. Shape memory and recovery quantification

Figure SI-6. Shape recovery illustration of PHU_{50} from ice bath to hot water bath.

Thermal expansion measurement and height recovery correction.

Thermal expansion of the PHU pastilles was determined by rheometry, using a temperature ramp from 0 °C to 80 °C at a rate of 3 °C/min. The normal force was kept at 0.5 N, in order to maintain the PHU sample on the geometry. The height of the sample (h) was measured as a function of temperature (Figure SI.6). The curve h = f(T) was fitted with a 5th degree polynomial.

Figure SI.7 (pink curve) represents the height h(T)-$h_{initial}$ of PHU_{100} pastille recovered over temperature, during the first shape recovery measurement cycle (Cycle 1), after compression (20 N) at 0 °C. As evidenced by the graph, the height recovery starts around 20 °C (value close to PHU_{100} T_g, i.e. 20 °C). After 45 °C, a slope change is observed (pink curve), showing that even at high temperature, the measured sample height is still increasing, suggesting that the shape recovery is not over. Nevertheless, upon application of the correction previously established, equation expressing PHU_{100} thermal expansion, i.e. height as a function of temperature (orange curve), a plateau is obtained after 45 °C. The previous observation shows that the height recovery is complete and stable above this temperature. This results show that first the thermoresponsive behavior of PHUs is driven by their T_g and second that 80 °C is an appropriate temperature to perform shape memory recovering tests.

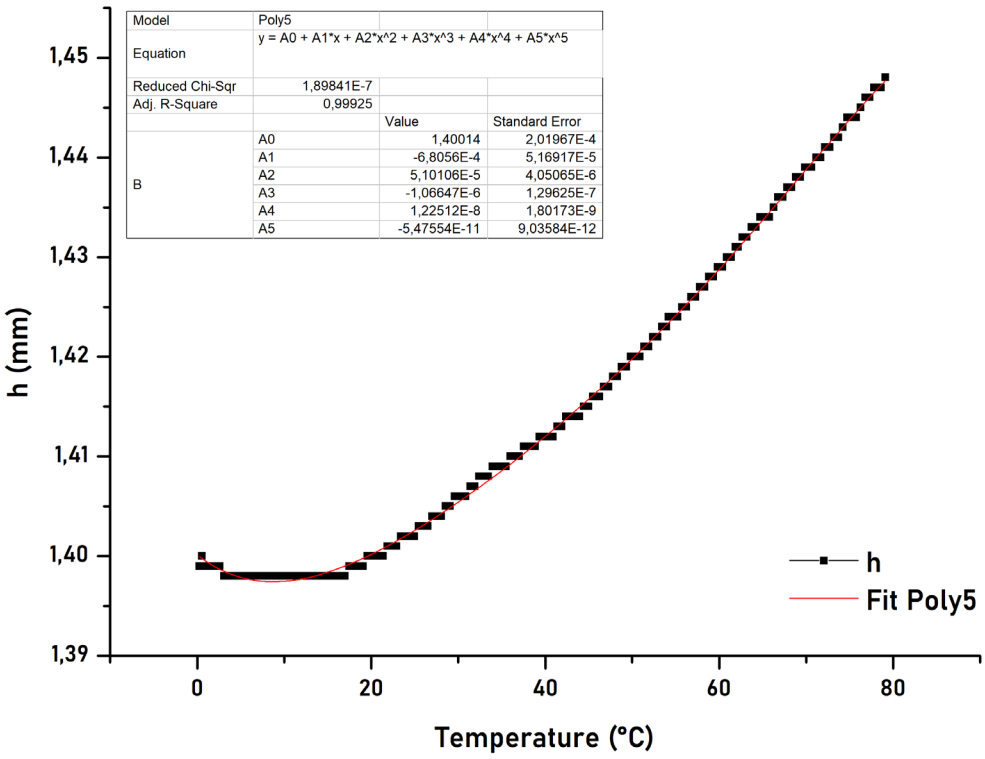

Figure SI-7. PHU_{100} thermal expansion measured with a temperature ramp from 0 °C to 80 °C at 3 °C/min and fitting with a 5th degree polynomial.

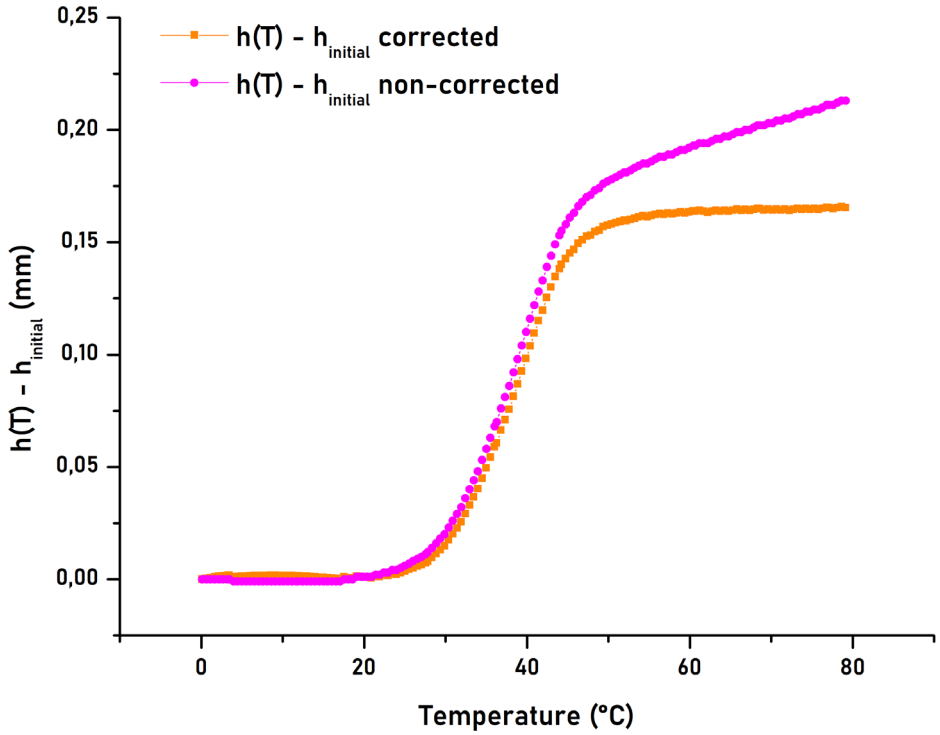

Figure SI-8. Evolution of height $h(t)-h_{initial}$ as a function of temperature for $PHUs_{0-100}$ (left) and correction example on PHU_{100} with thermal expansion removal.

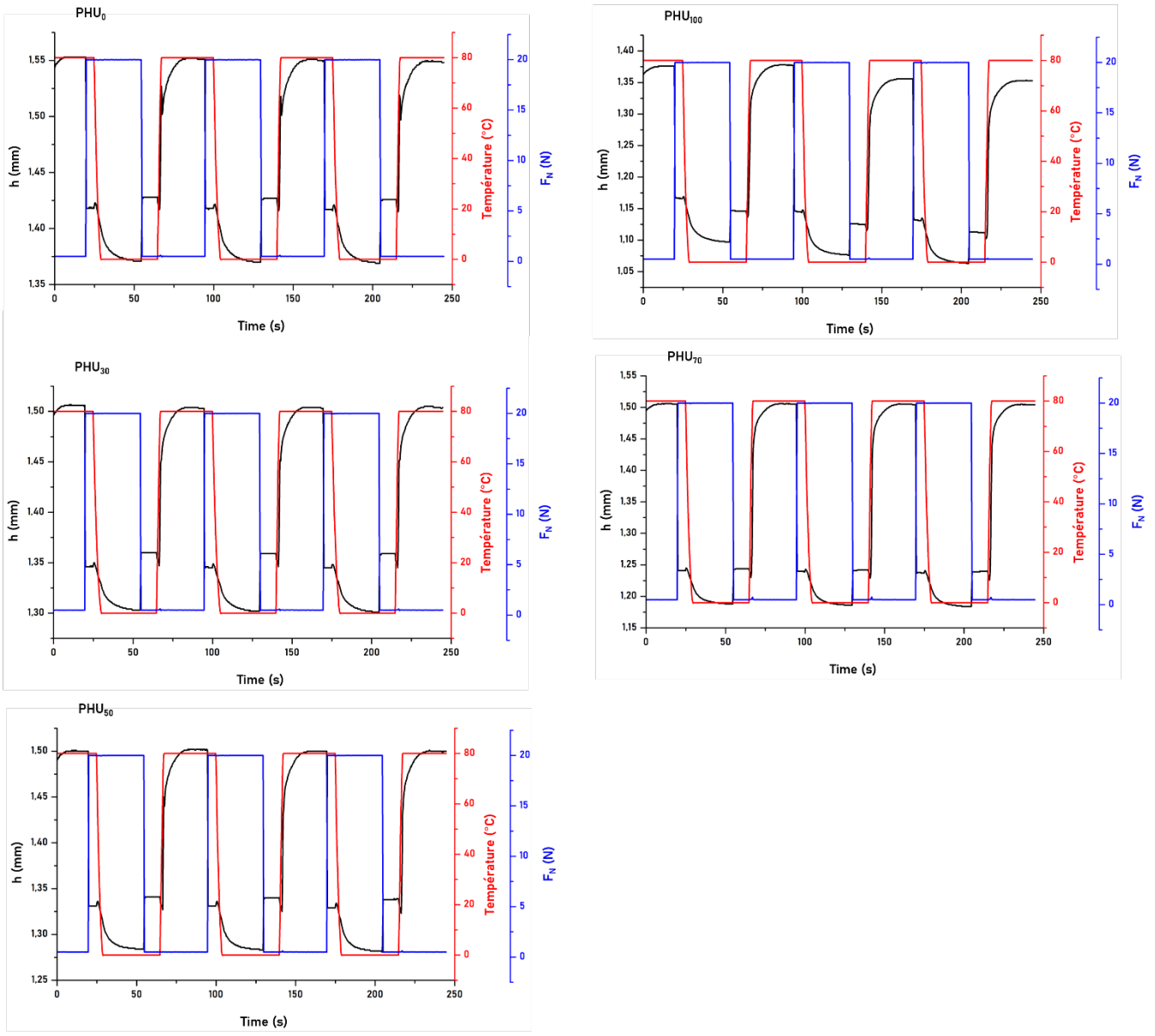

Figure SI-9. Thermo-responsive dual shape memory cycles 2, 3 and 4 of PHUs0-100, composed of h (black, sample height), FN (blue, normal force), and temperature (red) (a – e).

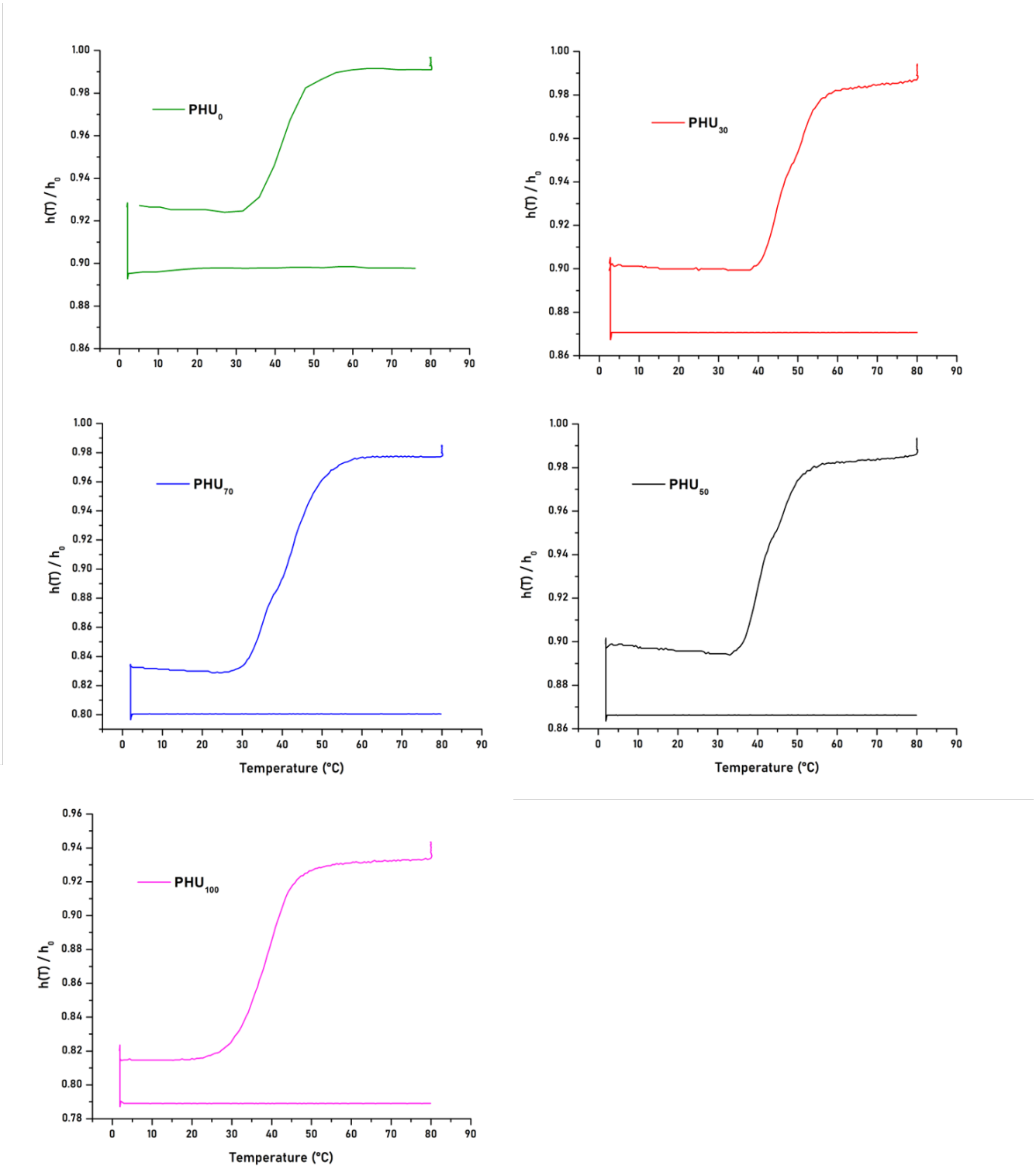

Figure SI-10. Variation of disk height during the first fixing and recovery steps of $PHUs_{0\text{-}100}$ with temperature ramps of 3 °C min^{-1}. Height values have been corrected with thermal expansion and normalized by sample initial heights.

Recovery at 37 °C.

The curves representing the $R_r(t)$ ratio are displayed in Figure 11 of the main paper text. The curves were fitted with the following equation:

$$y = A\, e^{\frac{-t}{\tau}} + y0$$

with A a pre-exponential factor, τ representing the relaxation time. The values of recovery ratio (and τ values) calculated after 1 or 2 hours are summarized in Table SI.3.
The calculation of relaxation times provides details about recovery kinetic, depending on the different amine ratio. Relaxation times obtained (Table SI.3) decrease when the TMAEA fraction is increasing (and $T_{\alpha\ decrease}$), showing that the kinetic of recovery is directly driven by the number of netpoints in the matrix: the higher the number of netpoints, the lower the mobility in the networks and the slower the recovery rate.

Table SI-3. Recovery ratio calculated for $PHUs_{0\text{-}100}$ after 1 h or 2 h at 37 °C, A, y0 and τ values obtained from the fitting equation and T_α values.

PHU	R_r ^{1h} (%)	R_r ^{2h} (%)	A	y_0	τ (s)	T_α (°C)
PHU_0	77	80	-57.6	78.5	814	47
PHU_{30}	76	Nd	Nd	Nd	Nd	42
PHU_{50}	86	87	-84.6	86.3	541	37
PHU_{70}	86	86	-88.2	86.0	423	36
PHU_{100}	80	80	-96.4	80.1	204	26

IV. PHU hydrolysis

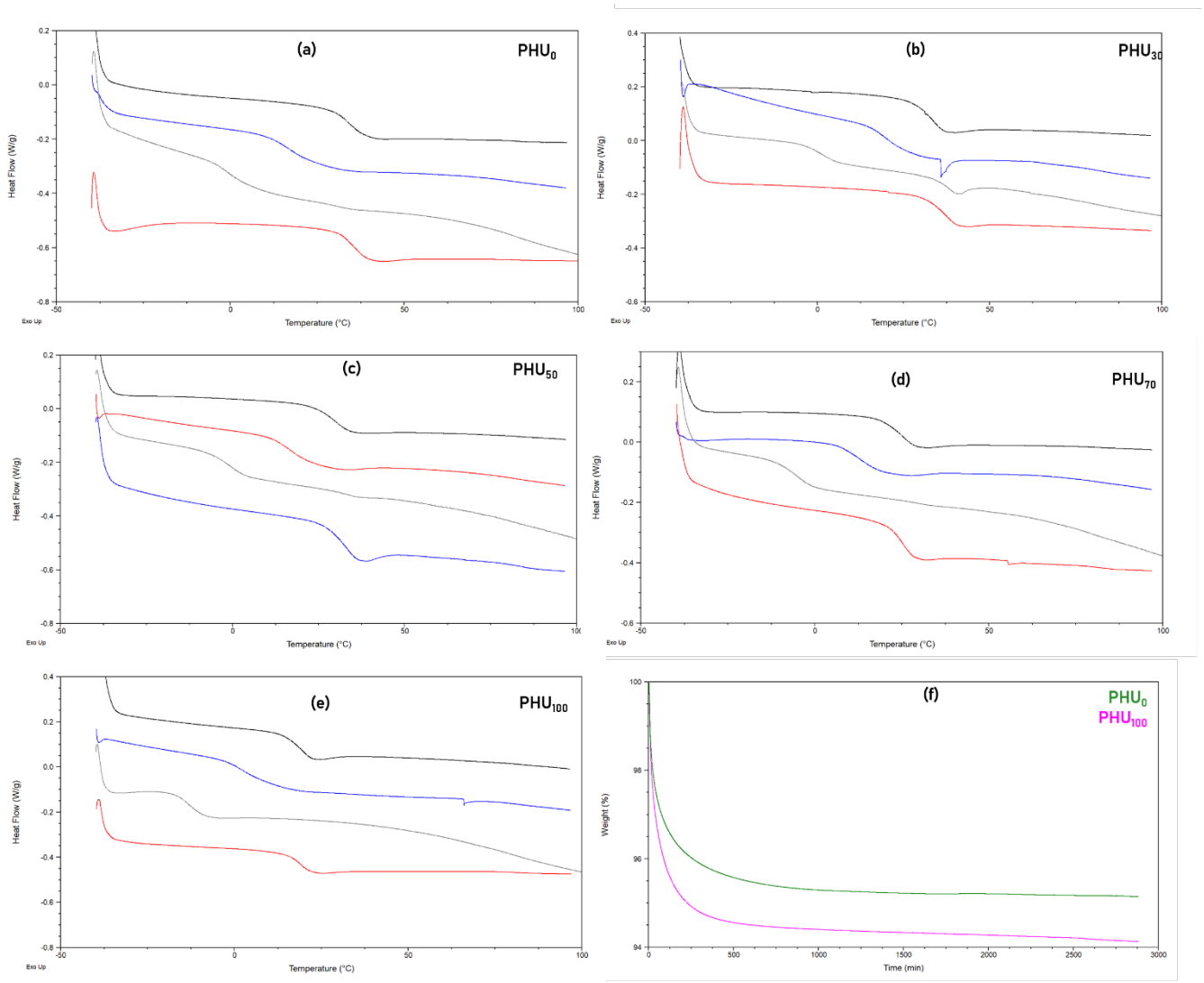

Figure SI-11. DSC first heating cycles of PHU_0 (a), PHU_{30} (b), PHU_{50} (c), PHU_{70} (d), PHU_{100} (e), initial sample (black curve), sample after 30 days in the open-air (grey), sample dried at 30 °C under vacuum (blue curve), and sample after 48 h drying at 80 °C (red). TGA traces obtained for PHU_0 (green curve) and PHU_{100} (pink curve) during 48 h isothermal analysis at 80 °C.

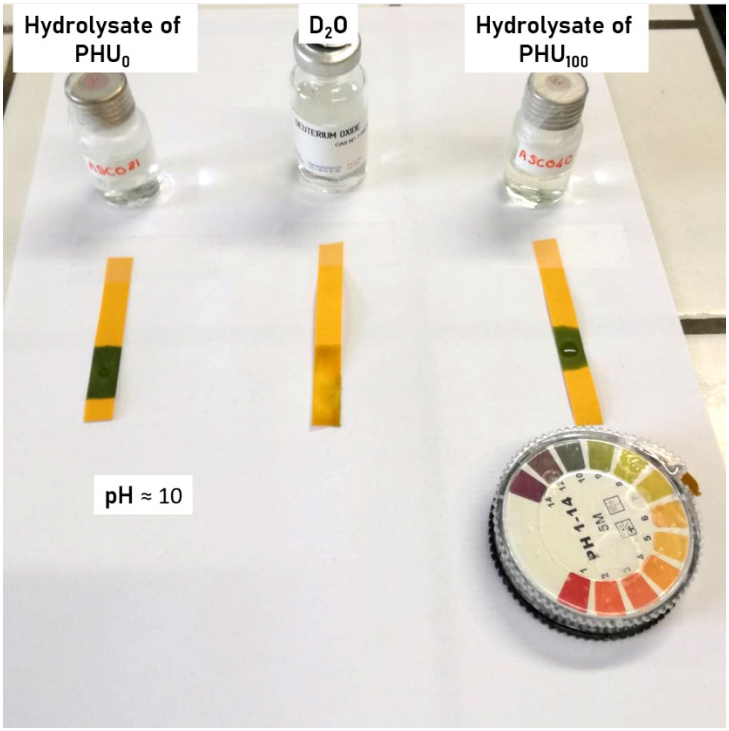

Figure SI-12. pH measurements on PHU_0 and PHU_{100} hydrolysates in D_2O.

HR-MAS analysis was performed on a piece of PHU0 swollen in DMSO-d6, in order to confirm the absence of proton belonging to urea moieties. Despite the relatively poor resolution of the resulting spectrum, the absence of signals near to classical urea shift (5.7 ppm) is clearly noticeable.

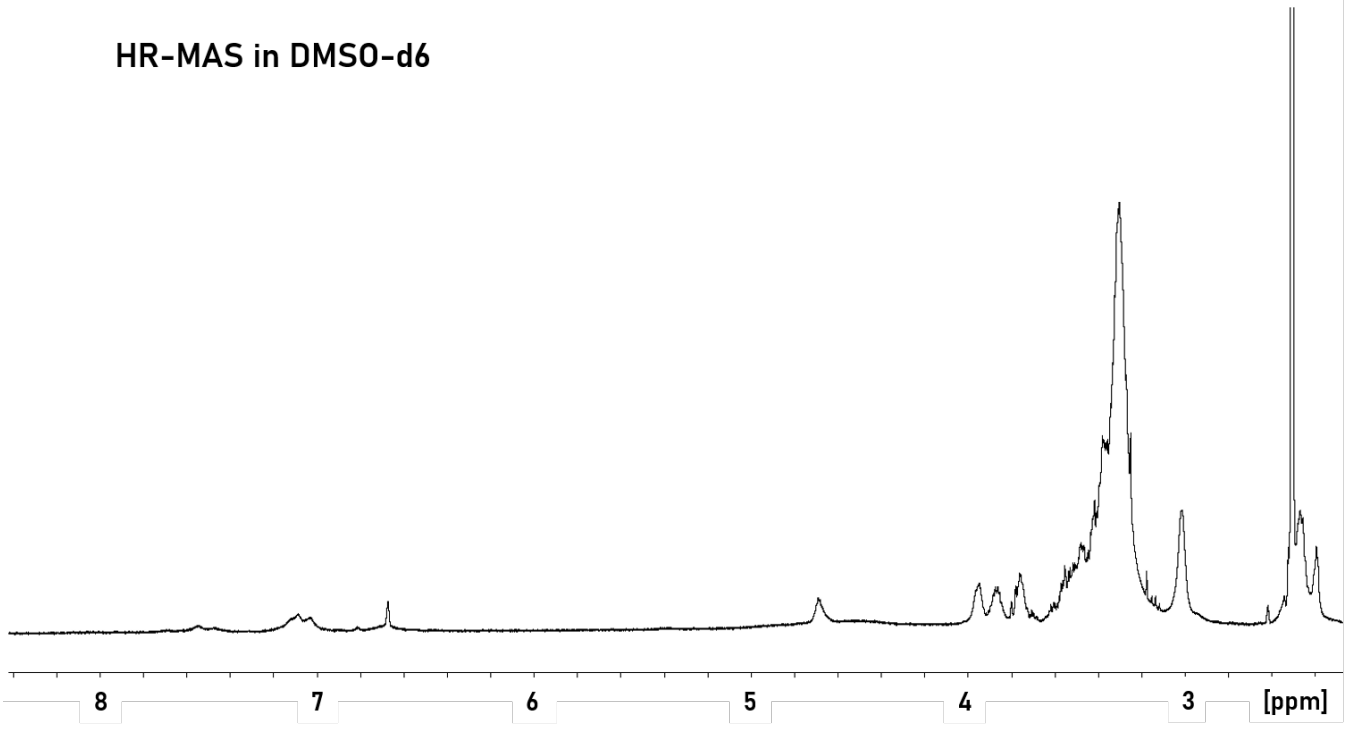

Figure SI-13. HR-MAS spectra of PHU0 swollen in DMSO-D6 at room temperature. Zoom between 2.4 and 8.4 ppm.

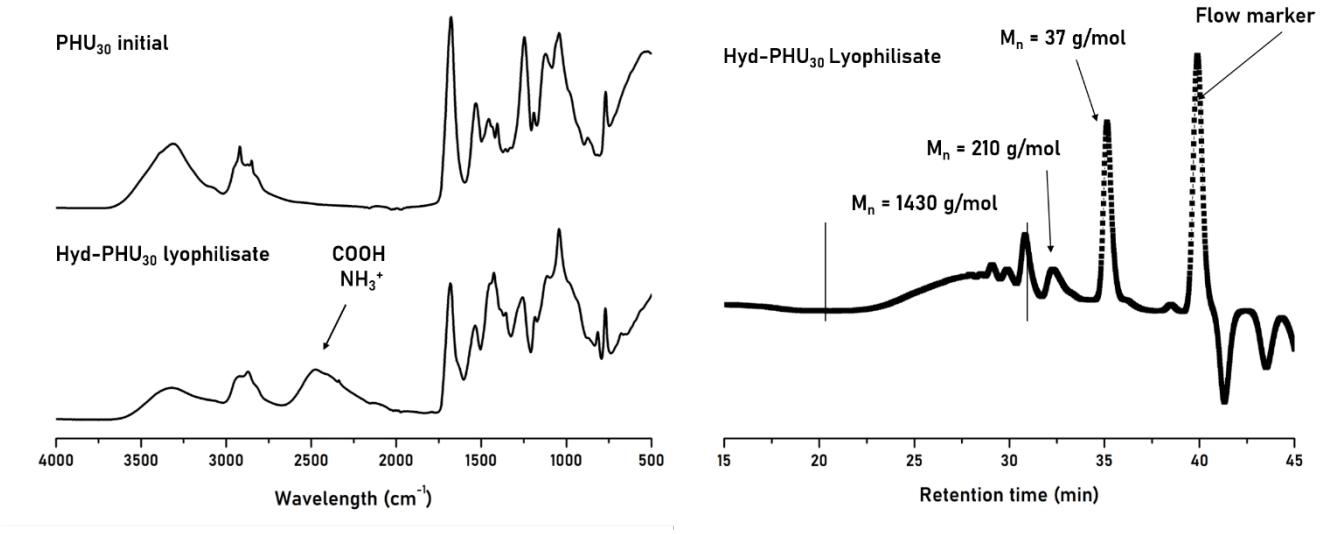

Figure SI-14. Stacked FTIR spectra of PHU_{30} initial pastille (up, left), and Hyd-PHU_{30} lyophilisate (bottom, left). SEC traces in DMF of Hyd-PHU_{30} lyophilisate.